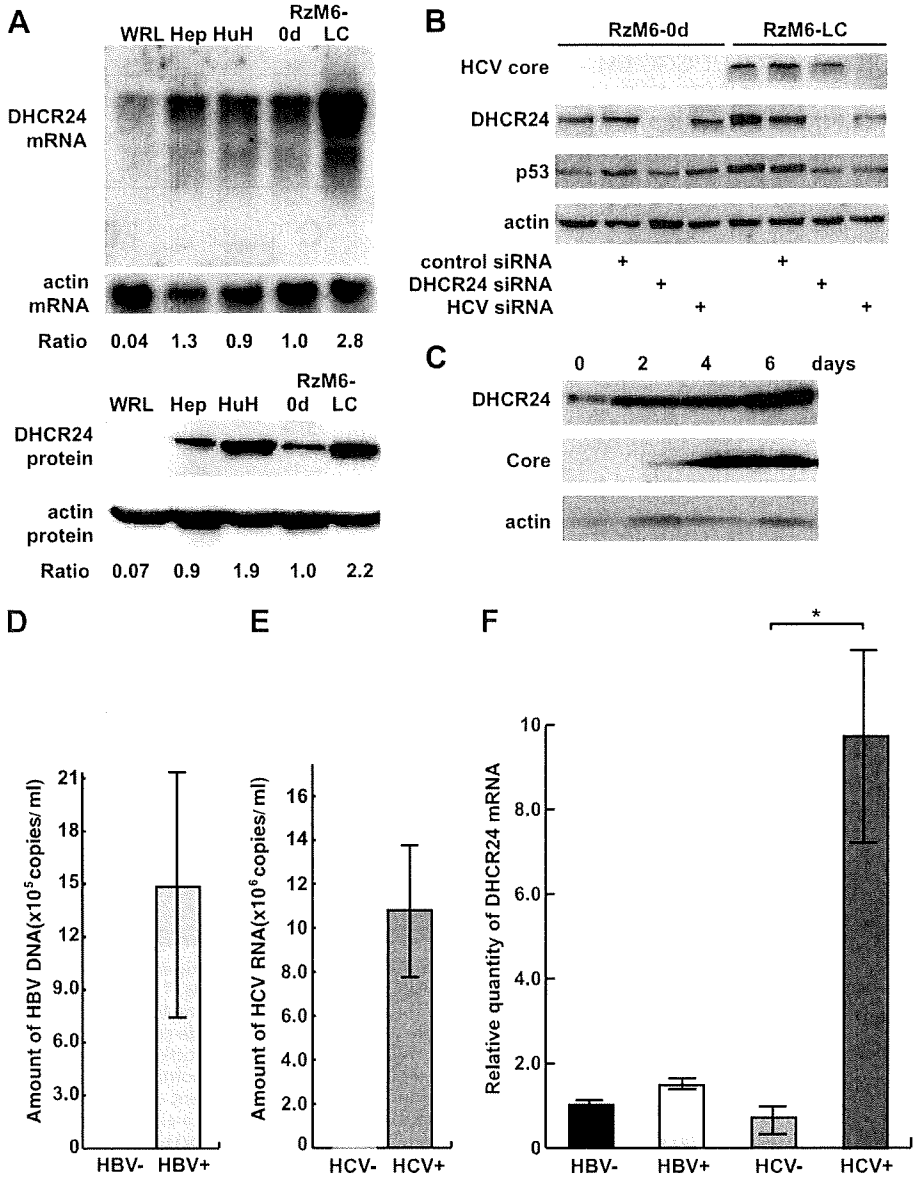

FIGURE 2. **Induction of DHCR24 by HCV in human liver cell lines.** *A*, expression of DHCR24 mRNA (Northern blot, *upper panel*) and protein (Western blot, *lower panel*) in WRL68 (*WRL*), HepG2 (*Hep*), HuH-7 (*HuH*), RzM6-0d, and RzM6-LC cells. Ratios indicate the amount of DHCR24 mRNA or protein in each cell type (quantified by densitometry) relative to that of RzM6-0d cells. *B*, Western blotting of HCV core protein, DHCR24, and p53 (DO-1 antibody) proteins in RzM6-0d and RzM6-LC cells following treatment with the indicated (+) siRNA. *C*, the induction of DHCR24 by HCV after 2, 4, and 6 days in RzM6 cells by treatment of tamoxifen (100 nM). Data are representative of two independent experiments, and anti-actin antibody was used as a loading control (*A–C*). *D*, amount of HBV DNA in HBV-infected human hepatocytes in chimeric mouse liver quantitated by RTD-PCR. *E*, amount of HCV-RNA in HCV-infected human hepatocytes in chimeric mouse liver quantitated by RTD-PCR. *F*, the quantitation of DHCR24 mRNA in mock-infected, HBV-infected, and HCV-infected human hepatocytes in chimeric mouse liver. *Vertical bars*, S.D.; *, $p < 0.05$ (two-tailed Student's *t* test).

protein and mRNA in a panel of hepatic and embryonic cell lines (Fig. 2*A*). Northern blotting revealed that DHCR24 mRNA expression was notably higher in RzM6-LC cells than in RzM6-0d cells, indicating that induction of DHCR24 occurs at the transcriptional level. DHCR24 protein levels were also higher in HuH-7 and RzM6-LC cells relative to RzM6-0d cells (Fig. 2*A*). To examine whether persistent up-regulation of *DHCR24* in RzM6-LC cells resulted from HCV expression, we utilized an siRNA to knockdown HCV expression (17) (Fig. 2*B*). Silencing HCV by greater than 99% with siRNA reduced the expression of DHCR24 and p53 in RzM6-LC cells. When we induced HCV expression with tamoxifen, the induction of DHCR24 was observed after 2, 4, and 6 days (Fig. 2*C*). These results indicate that expression of the full-length HCV genome induced DHCR24 overexpression. DHCR24 was not induced in HuH-7 cells infected with the HCV strain JFH-1 (22) (data not shown). This result might be explained by the substantial endogenous expression of DHCR24 in HuH-7 cells (Fig. 2*A* and supplemental Fig. 1*A*). To examine whether HCV infection can induce DHCR24, human hepatocytes in chimeric mice were infected with hepatitis B virus (HBV) or HCV (Fig. 2, *D* and *E*). Notable up-regulation of DHCR24 mRNA was detected in HCV-infected human hepatocytes but not in HBV-infected human hepatocytes (Fig. 2*F*).

Persistent Overexpression of DHCR24 Induces Apoptotic Resistance to Oxidative Stress—As HCV infection increased the expression of DHCR24, we further examined the effect of DHCR24 on hepatocytes. Because DHCR24 regulates oxidative stress-induced apoptosis (19, 21, 23, 24), the terminal deoxynucleotidyltransferase-mediated dUTP nick end labeling assay was performed with RzM6 cells to examine the effect of DHCR24 overexpression on H_2O_2-induced apoptosis (Fig. 3*A*). Fragmentation of genomic DNA was less pronounced in DHCR24-overexpressing cells (RzM6-LC cells and RzM6-0d cells transduced with DHCR24 lentivirus) than in RzM6-0d cells or RzM6-0d cells transduced with empty lentiviral vector. To quantify the apoptotic response, we examined the effect of DHCR24 overexpression on caspase activity (Fig. 3, *B–D*). Caspase activation by H_2O_2 was suppressed in RzM6-LC cells compared with RzM6-0d cells (Fig. 3*B*). Transfection with HCV siRNA recovered the caspase response in RzM6-LC cells. Caspase 3/7 activity was also examined following the transfection of HepG2 cells with pCA-Rz (Fig. 3*C*). Induction of caspase activation by H_2O_2 was inhibited by expression of the HCV gene; the inhibition was partially recovered by transfection with DHCR24

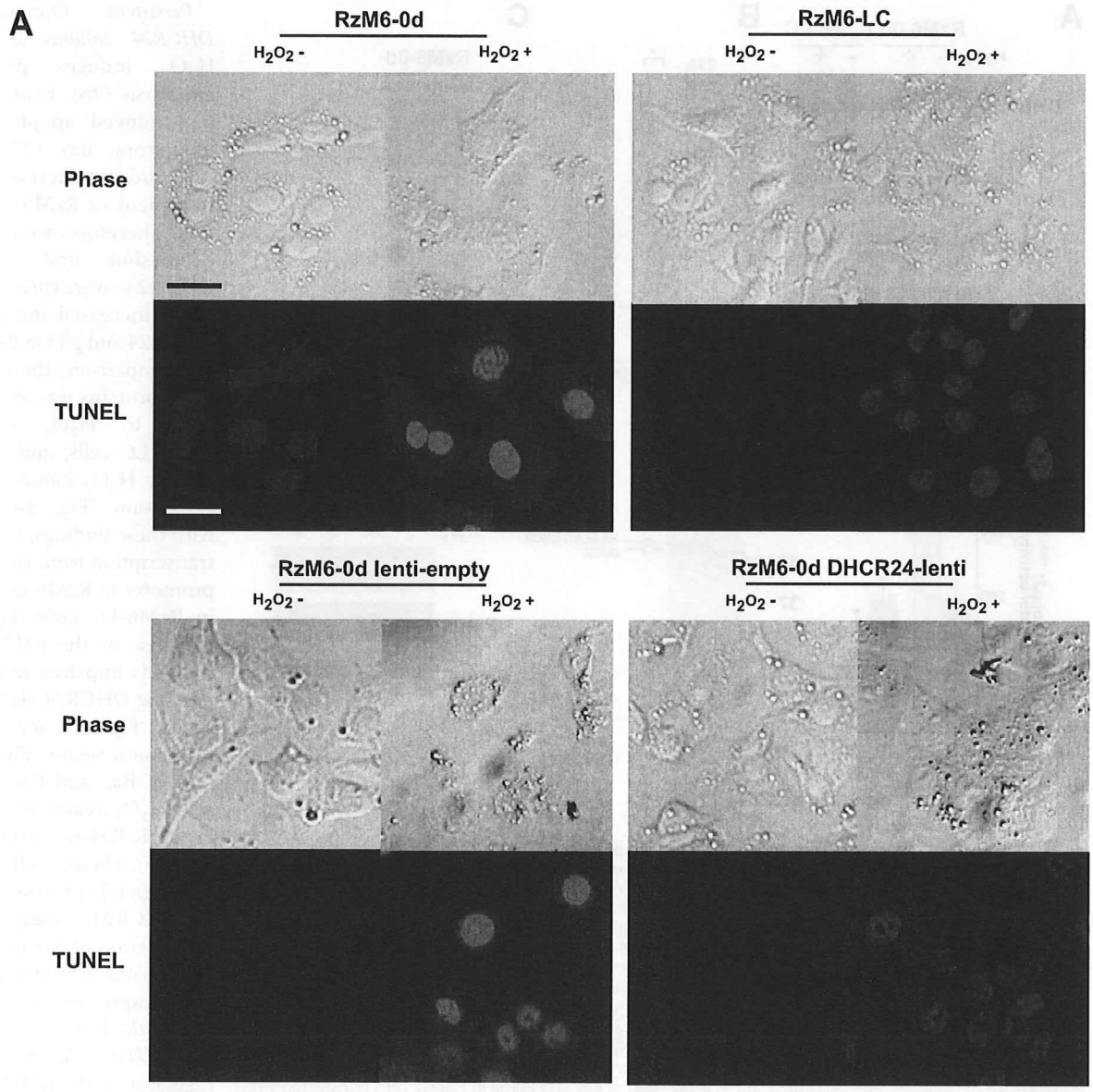

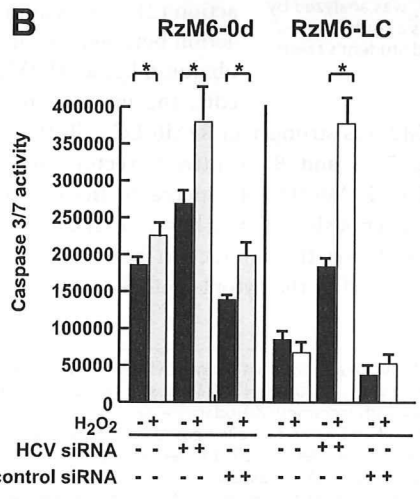

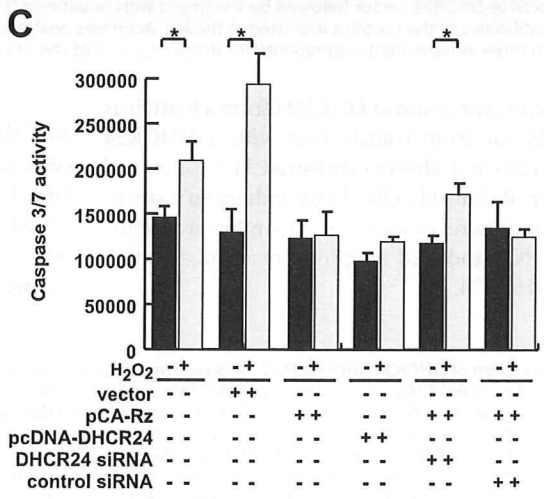

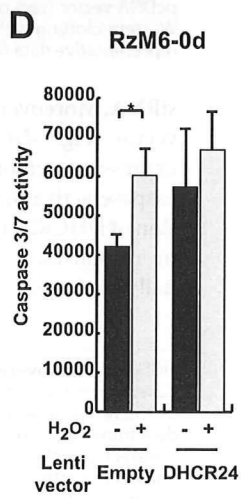

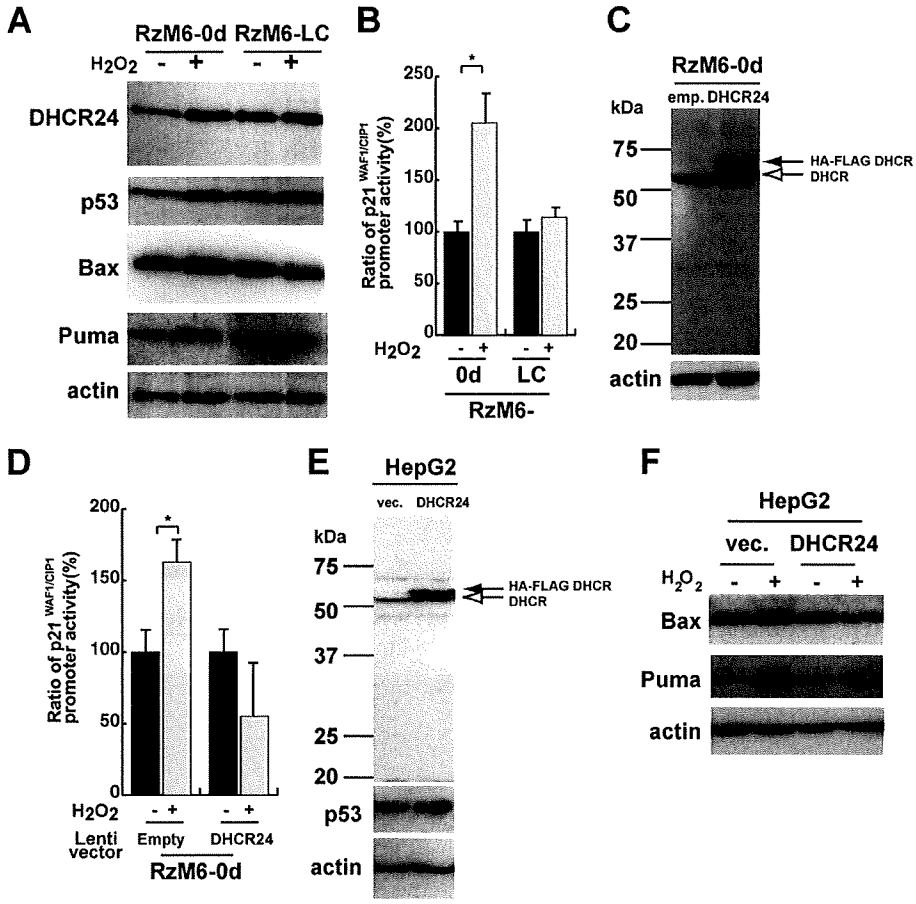

FIGURE 4. **Persistent overexpression of DHCR24 impairs p53 activity.** *A*, Western blotting of RzM6-0d and RzM6-LC cells treated with or without H_2O_2 was performed using antibodies against the proteins indicated on the *left*. *B*, p21$^{WAF1/CIP1}$ promoter activity in RzM6-0d and RzM6-LC cells transfected with pWWP-Luc followed by treatment with or without H_2O_2. Promoter activity was calculated as the ratio of firefly luciferase activity to *Renilla* luciferase activity. The ratio of promoter activity with H_2O_2 treatment to without H_2O_2 treatment is indicated as a percentage. *C*, DHCR24 expression in RzM6-0d cells transduced with lenti-empty (*emp.*) or lenti-DHCR24 (with HA-FLAG tag) vector. *D*, p21$^{WAF1/CIP1}$ promoter activity in RzM6-0d cells transfected with lenti-empty or lenti-DHCR24 vector followed by treatment with or without H_2O_2. Promoter activity was calculated as the ratio of firefly luciferase activity to *Renilla* luciferase activity. The ratio of promoter activity with H_2O_2 treatment to activity without H_2O_2 treatment is indicated as a percentage. *E*, HepG2 cells transfected with pcDNA vector (*vec*) or DHCR24 expression vector (pcDNA-DHCR24 HA-FLAG tag; *DHCR24*) and selected by G418 were analyzed by Western blotting with DHCR24 monoclonal antibody 2-152a (*top*), p53 monoclonal antibody (DO-1) (*middle*), and actin (*bottom*). *F*, expression of Bax and Puma in HepG2 cells transfected with pcDNA vector (*vec*) or pcDNA-DHCR24 vector followed by treatment with or without H_2O_2 was analyzed by Western blotting with antibodies to the proteins indicated at the *left*. Actin was analyzed as a control. In *A–F*, representative data from three independent experiments are shown; *, $p < 0.05$ (two-tailed Student's *t* test).

siRNA. Moreover, overexpression of DHCR24 from a lentivirus vector (Fig. 3*D*) (25) or from transfection with a DHCR24 expression vector (data not shown) impaired H_2O_2-induced caspase activation in RzM6-0d cells. Thus, enhanced expression of DHCR24 promotes resistance to H_2O_2-induced apoptotic responses, and HCV-induced apoptotic resistance is partially mediated by DHCR24.

Persistent Overexpression of DHCR24 Inhibits p53 Activity—H_2O_2 induces p53-dependent apoptosis (26). Expression of the p53-induced apoptotic response mediators, Bax (27) and Puma (28), did not increase after H_2O_2 treatment of RzM6-LC cells (Fig. 4*A*). Therefore, we examined p53 expression and function in DHCR24-overexpressing cells. H_2O_2 increased the expression of DHCR24 and p53 in RzM6-0d cells. By comparison, the expression of these proteins was already elevated prior to H_2O_2 treatment in RzM6-LC cells, and we found no further H_2O_2-induced increase in expression (Fig. 4*A*). Consistent with these findings, H_2O_2 activated transcription from the p21$^{WAF1/CIP}$ promoter in RzM6-0d cells but not in RzM6-LC cells (Fig. 4*B*). This response of the p21$^{WAF1/CIP}$ promoter is impaired in cells overexpressing DHCR24 via the lentivirus vector (Fig. 4, *C* and *D*) or via the expression vector (Fig. 4*E*). Induction of Bax and Puma expression after H_2O_2 treatment was decreased in DHCR24-overexpressing cells (Fig. 4*F*). These results indicate that although p53 expression is elevated in DHCR24-overexpressing cells, the function of p53 in the oxidative stress pathway is impaired.

Overexpression of DHCR24 Enhances the Interaction between p53 and MDM2—Since DHCR24 is a regulator of the p53-MDM2 interaction (21), we examined the interaction between p53 and its specific ubiquitin ligase, MDM2. Unexpectedly, the interaction between p53 and MDM2 was stronger in RzM6-LC cells than in RzM6-0d cells (Fig. 5, *A* and *B*). Lentiviral vector overexpression of DHCR24 in RzM6-0d cells increased the binding of p53 to MDM2 (data not shown). Furthermore, cell fractionation analysis revealed that the interaction between MDM2 and p53 mostly occurred in the cytoplasmic fraction, even after H_2O_2

FIGURE 3. **Prior overexpression of DHCR24 inhibits H_2O_2-induced apoptosis.** *A*, representative phase-contrast images of RzM6-0d and RzM6-LC cells (*upper panels*) or lenti-empty and lenti-DHCR24 vector-transduced RzM6-0d cells (*lower panels*) treated with or without H_2O_2 (1 mM, 4 h). *In situ* cell death was detected by the terminal deoxynucleotidyltransferase-mediated dUTP nick end labeling (*TUNEL*) assay with tetramethylrhodamine. *Scale bars*, 25 nm. Representative data from three experiments are shown. *B*, caspase 3/7 activity (relative light units) in RzM6-0d and RzM6-LC cells treated with or without H_2O_2. Cells were transfected with or without HCV siRNA or with control siRNA as indicated. *C*, caspase 3/7 activity in HepG2 cells treated with or without H_2O_2. Cells were transfected with control pcDNA vector (vector), pCA-Rz, pcDNA-DHCR24, DHCR24 siRNA, or control siRNA. *D*, caspase 3/7 activity in RzM6-0d cells treated with or without H_2O_2. Cells were transduced with lenti-empty or lenti-DHCR24 vector. In *B–D*, data reflect the means ± S.D. of three independent triplicate experiments; *, $p < 0.05$ (two-tailed Student's *t* test).

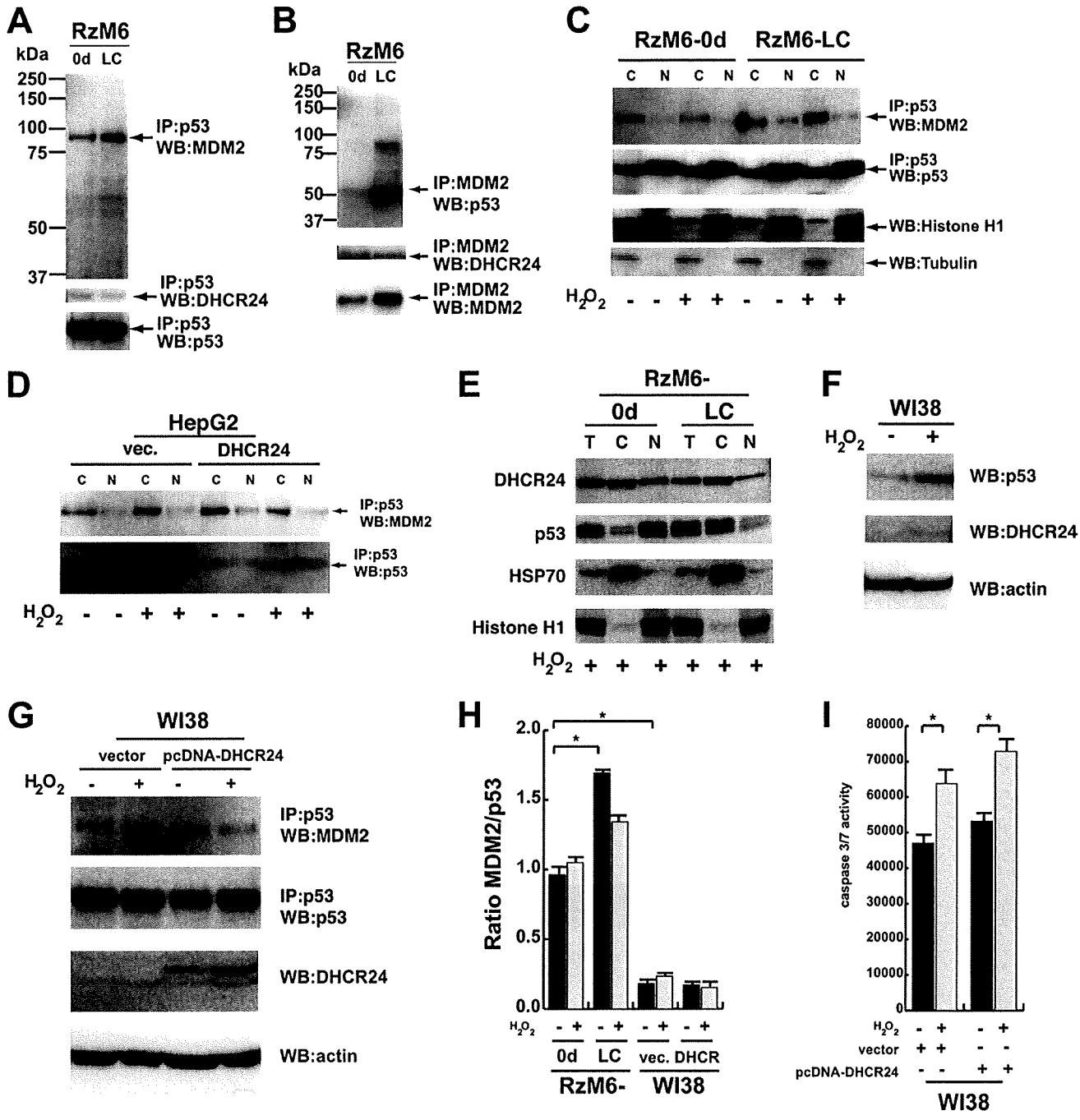

FIGURE 5. **DHCR24 overexpression enhances the interaction between p53 and MDM2 in the cytoplasm.** *A*, p53 was immunoprecipitated (*IP*) from RzM6-0d and RzM6-LC cells with polyclonal anti-p53 antibody (FL393) followed by Western blotting with monoclonal antibodies against MDM2 (*top*) and p53 or DHCR24 (*bottom*). *B*, MDM2 was immunoprecipitated from RzM6-0d and RzM6-LC cells using polyclonal anti-MDM2 antibody (H221) followed by Western blotting (*WB*) with monoclonal antibodies against p53 (*top*) and MDM2 or DHCR24 (*bottom*). *C*, p53 was immunoprecipitated from cytoplasmic (C) or nuclear (*N*) fractions of RzM6-0d and LC cells using anti-p53 antibody (FL393) followed by Western blotting with anti-MDM2 antibody (*top*) and anti-p53 antibody (*bottom*). Cell fractionation was confirmed by Western blotting with anti-histone H1 and tubulin (*WB*). *D*, p53 was immunoprecipitated from cytoplasmic or nuclear fractions of HepG2 cells transfected with control pcDNA (*vec*) or pcDNA-DHCR24 expression vector using polyclonal anti-p53 (FL393) followed by Western blotting with antibodies against the proteins indicated at the right. Reaction with secondary antibodies (anti-rabbit or mouse IgG conjugated with horseradish peroxidase) alone did not show any signal (data not shown), and data representative of three independent experiments are shown (*A–D* and *G*). *E*, RzM6-0d or RzM6-LC cells with H_2O_2 treatment were fractionated into total (*T*), cytoplasmic, and nuclear fractions and subjected to Western blotting with the antibodies indicated on the *left*. *F*, Western blotting of WI38 cells with or without H_2O_2 treatment (0.5 mM, 4 h) with antibodies against p53, DHCR24, and actin. *G*, immunoprecipitation of p53 from cells transfected with pcDNA vector and pcDNA-DHCR24 (*DHCR*) with or without H_2O_2 treatment (0.5 mM, 4 h), followed by Western blotting with antibodies against MDM2 (*first column*) and p53 (*second column*). Cells were examined with Western blotting with anti-DHCR24 (*third column*) and anti-actin (*fourth column*). *H*, the average ratio of the quantified results of immunoprecipitation of p53 and Western blotting of MDM2 in RzM6-0d, RzM6-LC, and WI38 cells with transfection of pcDNA vector or pcDNA-DHCR24 with or without H_2O_2 treatment are indicated. *Vertical bars*, S.D. *, $p < 0.05$ (two-tailed Student's *t* test). *I*, a caspase 3/7 assay was performed in WI38 cells with pcDNAvector (vector) and pcDNA-DHCR24 overexpression vector. *Vertical bars*, S.D. *, $p < 0.05$ (two-tailed Student's *t* test).

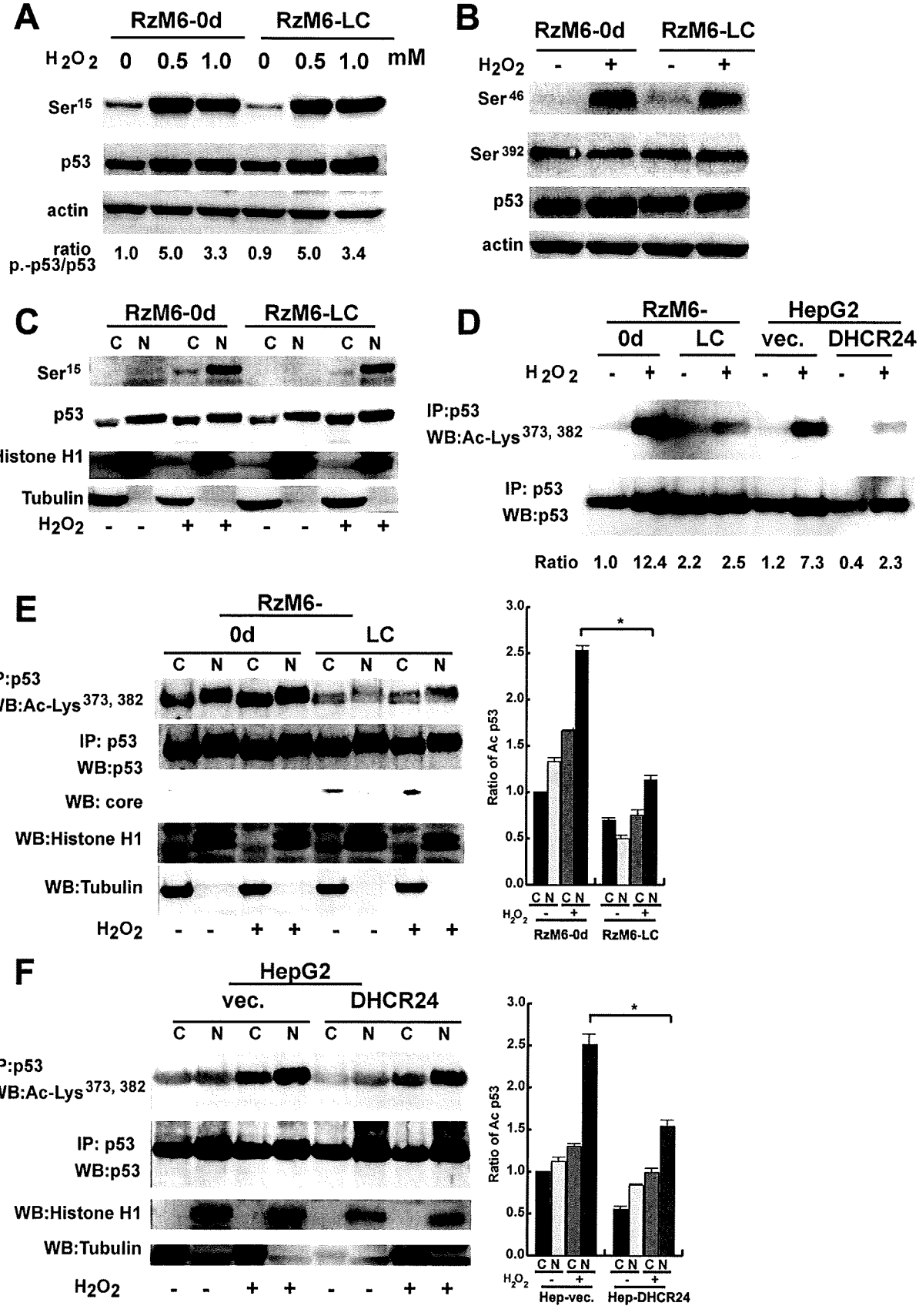

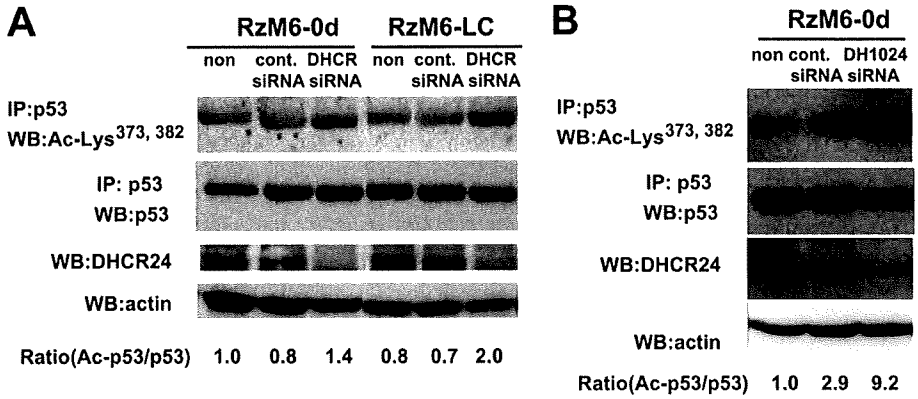

FIGURE 7. **Silencing of DHCR24 increases p53 acetylation.** *A*, RzM6-0d and RzM6-LC cells were untreated (*non*) or treated with control siRNA (*cont. siRNA*) or DHCR24 siRNA. Acetylated p53 Lys^{373} and Lys^{382} (*top*) and total p53 (*bottom*) were immunoprecipitated (*IP*) with anti-p53 antibody (*DO-1*) followed by Western blotting (*WB*), and the expression of actin and DHCR24 by Western blotting (*bottom*) was examined. The average ratio of acetylated p53 to total p53 in RzM6-0d cells without treatment is indicated at the *bottom*. *B*, RzM6-0d cells were transfected with control siRNA (*cont.siRNA*), DHCR24 siRNA (*DH1024* or *DHCR*), or untreated (*non*). Acetylated p53 Lys^{373} and Lys^{382} (*top*) and total p53 (*bottom*) were immunoprecipitated with anti-p53 antibody followed by Western blotting, and the expression of actin and DHCR24 by Western blotting (*bottom*) was examined. Reaction with secondary antibodies (anti-rabbit or mouse IgG conjugated with horseradish peroxidase) alone did not yield any signals (data not shown), and data representative of three independent experiments are shown (*A* and *B*).

treatment (Fig. 5*C*). Silencing of DHCR24 with siRNA decreased the interaction between p53 and MDM2 (supplemental Fig. 2*A*). Overexpression of DHCR24 in HepG2 cells increased the interaction between p53 and MDM2 in the cytoplasm (HepG2-DHCR24; Fig. 5*D* and supplemental Fig. 2, *B* and *C*). Level of p53 in the nucleus after treatment with H_2O_2 was low in RzM6-LC cells (Fig. 5*E*).

In a previous *in vitro* study that used bacterially expressed and purified protein (21), the interaction between p53 and MDM2 was decreased when the amount of DHCR24 was increased. These discrepancies with our results may be due to the different experimental systems. p53 and DHCR24 were induced by H_2O_2 in WI38TERT cells (21), as observed in our system (Fig. 5*F*). However, the interaction between MDM2 and p53 was much lower in WI38 cells than in RzM6 cells (Fig. 5, *G* and *H*). Moreover, ectopic expression of DHCR24 did not inhibit apoptotic response to H_2O_2 in WI38 cells (Fig. 5*I*) but suppressed apoptosis in HepG2 cells (Fig. 3). This different response may be due to the different regulatory systems of p53 and MDM2 in the liver and lung; MDM2 phosphorylation at Ser^{166} is regulated by the MEK-ERK (mitogen-activated protein kinase/extracellular signal-regulated kinase kinase-extracellular signal-regulated kinase) pathway in hepatocytes and Akt in lung cells (29). The response of MDM2 at Ser^{166} to H_2O_2 was significantly high in liver (HepG2) cells but was low in WI38 cells (supplemental Fig. 2, *D* and *E*), as previously observed in A549 cells (29). The up-regulation of MDM2 phosphorylation at Ser^{166} accelerates its E3 ligase activity (30).

We also found that overexpression of DHCR24 did not up-regulate the transcription of *p53* or *MDM2* genes (supplemental Fig. 3, *A* and *B*). However, DHCR24 overexpression inhibited polyubiquitination in RzM6-LC cells and H358 (p53 null) cells (supplemental Fig. 3, *C–E*). This inhibition of polyubiquitination would inhibit p53 degradation, resulting in an increased amount of p53 available to interact with MDM2.

Posttranslational Modification of p53 in DHCR24-overexpressing Cells—We did not detect any *p53* nucleotide substitutions in RzM6-LC cells compared with the *p53* in RzM6-0d cells (data not shown). Thus, we examined the posttranslational modification of p53, which is thought to be tightly connected to the regulation of its function and localization (31). We examined the phosphorylation of p53 at Ser^{15} (Fig. 6*A*); at Ser^{6}, Ser^{9}, Ser^{20}, and Ser^{37} (supplemental Fig. 4*A*); and at Ser^{46} and Ser^{392} (Fig. 6*B*) by Western blotting and found no marked differences in phosphorylation after H_2O_2 treatment between RzM6-0d and RzM6-LC cells. Ser^{15}-phosphorylated p53 was detected in the nuclear fraction of RzM6-0d and RzM6-LC cells after H_2O_2 treatment (Fig. 6*C*). We assessed the acetylation of p53 at Lys^{373} and Lys^{382} by immunoprecipitation followed by Western blotting and found that acetylation of p53 was significantly low in RzM6-LC cells compared with RzM6-0d cells following H_2O_2 treatment (Fig. 6*D*). H_2O_2 induced the acetylation of p53 at Lys^{373} and Lys^{382} in RzM6-0d cells (Fig. 6*E*). This acetylation

FIGURE 6. **Posttranslational modification of p53 in cells overexpressing DHCR24.** *A*, phosphorylation of p53 at Ser^{15} in RzM6-0d and RzM6-LC cells after treatment with 0, 0.5, or 1.0 mM H_2O_2 was examined by Western blotting with specific rabbit polyclonal antibodies. p53 was detected with anti-p53 monoclonal antibody (*DO-1*). Actin was analyzed as a control. *B*, phosphorylation of p53 at Ser^{46} and Ser^{392} in RzM6-0d and RzM6-LC cells after treatment with 0 or 1.0 mM H_2O_2 was analyzed by Western blotting with specific rabbit polyclonal antibodies. p53 was detected with anti-p53 monoclonal antibody. Actin was analyzed as a control. *C*, RzM6-0d or RzM6-LC cells with or without H_2O_2 treatment were fractionated into cytoplasmic (*C*) and nuclear (*N*) fractions that were subjected to Western blotting with the antibodies indicated on the *left*. *D*, acetylation of p53 Lys^{373} and Lys^{382} (*top*) and total p53 (*bottom*) was characterized by immunoprecipitation (*IP*) with anti-p53 antibody followed by Western blotting (*WB*) with the rabbit polyclonal antibodies indicated on the *left* in RzM6-0d and RzM6-LC cells or HepG2 cells transfected with pcDNA vector (*vec.*) or pcDNA-DHCR24 expression vector (*DHCR24*). The average ratio of acetylated p53 to total p53 in RzM6-0d cells without H_2O_2 treatment is indicated at the *bottom*. *E*, acetylation of p53 Lys^{373} and Lys^{382} (*top*) and total p53 (*second panel*) was characterized by immunoprecipitation with anti-p53 antibody followed by Western blotting with the rabbit polyclonal antibodies indicated on the *left* in RzM6-0d and RzM6-LC cells. HCV core protein was detected by Western blotting with monoclonal antibody (31, 32). Cell fractionation was confirmed with antibodies against histone H1 and tubulin. p53 and acetylated p53 were quantitated, and the average ratio of acetylated p53 to total p53 in the cytoplasmic (*C*) fraction of RzM6-0d cells is indicated. *Vertical bars*, S.D. *, $p < 0.05$ (two-tailed Student's *t* test). *F*, acetylation of p53 Lys^{373} and Lys^{382} (*top*) and total p53 (*second panel*) was characterized by IP with anti-p53 antibody followed by Western blotting with the rabbit polyclonal antibodies indicated on the *left* in HepG2 cells transfected with pcDNA vector or pcDNA-DHCR24 vector with or without H_2O_2 treatment. Cell fractionation was confirmed with antibodies against histone H1 and tubulin. p53 and acetylated p53 were quantitated, and the average ratio of acetylated p53 to total p53 in the cytoplasmic fraction of Hep-vec cells is indicated. *Vertical bars*, S.D. *, $p < 0.05$ (two-tailed Student's *t* test). Reaction with secondary antibodies (anti-rabbit or mouse IgG conjugated with horseradish peroxidase) alone did not show any signals (data not shown), and data representative of three independent experiments are indicated (*A–F*).

was significantly inhibited in RzM6-LC cells (Fig. 6*E*). Persistent ectopic overexpression of DHCR24 also repressed H_2O_2-induced p53 acetylation in the nuclei of HepG2 cells (Fig. 6*F*). In addition, silencing of DHCR24 by siRNA caused up-regulation of p53 acetylation at Lys^{373} and Lys^{382} in RzM6-0d and RzM6-LC cells (Fig. 7*A*). When the alternative siRNA for DHCR24 (DH1024) was transfected into RzM6-0d cells, the acetylation of p53 was accelerated (Fig. 7*B*). The mutant DHCR24 vector suppressed the effect of DHCR24 siRNA (supplemental Fig. 4*B*). These results indicate that overexpression of DHCR24 down-regulates p53 acetylation.

DISCUSSION

This study demonstrates that DHCR24 expression parallels hepatocarcinogenesis and that HCV induces overexpression of DHCR24 at both the mRNA and protein levels. Moreover, persistent DHCR24 overexpression suppresses the p53 response to H_2O_2. These findings are consistent with the previous report that inactivation and mutation of p53 plays a role in the development of HCC (32). Hepatocytes with p53 abnormalities are likely to escape from cell cycle check points and acquire resistance to apoptosis, thereby increasing their tumorigenic potential. Likewise, genetic inactivation of p53 is associated with late stage disease (32). HCV RNA levels are notably lower in cancerous tissues from HCV-positive HCC patients than in non-cancerous tissues (33). Thus, impairment of p53 function by HCV-induced DHCR24 overexpression might play a crucial role in early stage disease progression.

In DHCR24-overexpressing cells, p53 was mostly distributed in the cytoplasm (supplemental Fig. 2, *A* and *B*). This change in the distribution pattern of p53 might be caused by an increased interaction between p53 and MDM2, which might be induced by increased phosphorylation of MDM2 and suppression of polyubiquitination by overexpression of DHCR24. The up-regulation of the p53-MDM2 interaction negatively regulates p53 and shuttles p53 from the nucleus to the cytoplasm (34, 35). MDM2 inhibits both *p53* transcriptional activation and p300-mediated p53 acetylation upon ternary complex formation with p300 and p53 (36–38). Acetylation of p53 by CBP/p300 mostly occurs in the nucleus (36). Therefore, the increase in cytoplasmic p53-MDM2 complexes in DHCR24-overexpressing cells may account for the observed suppression of p53 acetylation in the nucleus, even after treatment with H_2O_2 (supplemental Fig. 5). Impaired acetylation of C-terminal lysine residues decreases the sequence-specific DNA-binding activity (39) and the stability of p53 (37, 40). Taken together, our data suggest that DHCR24 overexpression may down-regulate p53 function by inhibiting degradation, increasing the formation of the p53-MDM2 complex in the cytoplasm, and suppressing acetylation of p53 in the nucleus.

In conclusion, we propose that HCV infection impairs the function of p53 through DHCR24 overexpression, which up-regulates the interaction between p53 and MDM2 in the cytoplasm and suppresses p53 acetylation in the nucleus. Because overexpression of DHCR24 is observed in other cancers, including melanoma (24) and prostate cancer (41), the findings from this study might provide a foundation for investigations into the mechanisms underlying the formation of these cancers. We plan to examine the liver-specific regulatory network of the p53-MDM2 interaction by DHCR24 in a future study.

Acknowledgments—We thank S. Imajoh-Ohmi, H. Fukuda, T. Watanabe, S. Nakagawa, K. Tanaka, and R. Takehara for technical support and N. Sonenberg, Y. Furuichi, T. Tsukiyama, S. Tone, S. Sekiguchi, and F. Yasui for valuable comments. We thank S. Harada (Kumamoto University) for kind encouragement.

REFERENCES

1. Choo, Q. L., Kuo, G., Weiner, A. J., Overby, L. R., Bradley, D. W., and Houghton, M. (1989) *Science* **244,** 359–362
2. Tsukiyama-Kohara, K., Iizuka, N., Kohara, M., and Nomoto, A. (1992) *J. Virol.* **66,** 1476–1483
3. Grakoui, A., Wychowski, C., Lin, C., Feinstone, S. M., and Rice, C. M. (1993) *J. Virol.* **67,** 1385–1395
4. Pekow, J. R., Bhan, A. K., Zheng, H., and Chung, R. T. (2007) *Cancer* **109,** 2490–2496
5. Lauer, G. M., and Walker, B. D. (2001) *N. Engl. J. Med.* **345,** 41–52
6. Saito, I., Miyamura, T., Ohbayashi, A., Harada, H., Katayama, T., Kikuchi, S., Watanabe, Y., Koi, S., Onji, M., Ohta, Y., *et al.* (1990) *Proc. Natl. Acad. Sci. U.S.A.* **87,** 6547–6549
7. Shepard, C. W., Finelli, L., and Alter, M. J. (2005) *Lancet Infect. Dis.* **5,** 558–567
8. Kiyosawa, K., Umemura, T., Ichijo, T., Matsumoto, A., Yoshizawa, K., Gad, A., and Tanaka, E. (2004) *Gastroenterology* **127,** S17–S26
9. Parkin, D. M. (2001) *Lancet Oncol.* **2,** 533–543
10. Hussain, S. P., Schwank, J., Staib, F., Wang, X. W., and Harris, C. C. (2007) *Oncogene* **26,** 2166–2176
11. Tardif, K. D., Waris, G., and Siddiqui, A. (2005) *Trends Microbiol.* **13,** 159–163
12. Levrero, M. (2006) *Oncogene* **25,** 3834–3847
13. Tsukiyama-Kohara, K., Toné, S., Maruyama, I., Inoue, K., Katsume, A., Nuriya, H., Ohmori, H., Ohkawa, J., Taira, K., Hoshikawa, Y., Shibasaki, F., Reth, M., Minatogawa, Y., and Kohara, M. (2004) *J. Biol. Chem.* **279,** 14531–14541
14. Köhler, G., and Milstein, C. (1975) *Nature* **256,** 495–497
15. Yasui, K., Wakita, T., Tsukiyama-Kohara, K., Funahashi, S. I., Ichikawa, M., Kajita, T., Moradpour, D., Wands, J. R., and Kohara, M. (1998) *J. Virol.* **72,** 6048–6055
16. Tsukiyama-Kohara, K., Poulin, F., Kohara, M., DeMaria, C. T., Cheng, A., Wu, Z., Gingras, A. C., Katsume, A., Elchebly, M., Spiegelman, B. M., Harper, M. E., Tremblay, M. L., and Sonenberg, N. (2001) *Nat. Med.* **7,** 1128–1132
17. Watanabe, T., Sudoh, M., Miyagishi, M., Akashi, H., Arai, M., Inoue, K., Taira, K., Yoshiba, M., and Kohara, M. (2006) *Gene. Ther.* **13,** 883–892
18. Iivonen, S., Hiltunen, M., Alafuzoff, I., Mannermaa, A., Kerokoski, P., Puoliväli, J., Salminen, A., Helisalmi, S., and Soininen, H. (2002) *Neuroscience* **113,** 301–310
19. Greeve, I., Hermans-Borgmeyer, I., Brellinger, C., Kasper, D., Gomez-Isla, T., Behl, C., Levkau, B., and Nitsch, R. M. (2000) *J. Neurosci.* **20,** 7345–7352
20. Waterham, H. R., Koster, J., Romeijn, G. J., Hennekam, R. C., Vreken, P., Andersson, H. C., FitzPatrick, D. R., Kelley, R. I., and Wanders, R. J. (2001) *Am. J. Hum. Genet.* **69,** 685–694
21. Wu, C., Miloslavskaya, I., Demontis, S., Maestro, R., and Galaktionov, K. (2004) *Nature* **432,** 640–645
22. Wakita, T., Pietschmann, T., Kato, T., Date, T., Miyamoto, M., Zhao, Z., Murthy, K., Habermann, A., Kräusslich, H. G., Mizokami, M., Bartenschlager, R., and Liang, T. J. (2005) *Nat. Med.* **11,** 791–796
23. Kuehnle, K., Crameri, A., Kälin, R. E., Luciani, P., Benvenuti, S., Peri, A., Ratti, F., Rodolfo, M., Kulic, L., Heppner, F. L., Nitsch, R. M., and Mohajeri, M. H. (2008) *Mol. Cell. Biol.* **28,** 539–550
24. Di Stasi, D., Vallacchi, V., Campi, V., Ranzani, T., Daniotti, M., Chiodini, E., Fiorentini, S., Greeve, I., Prinetti, A., Rivoltini, L., Pierotti, M. A., and Rodolfo, M. (2005) *Int. J. Cancer* **115,** 224–230
25. Lois, C., Hong, E. J., Pease, S., Brown, E. J., and Baltimore, D. (2002) *Science*

295, 868–872
26. Yamamoto, H., Ozaki, T., Nakanishi, M., Kikuchi, H., Yoshida, K., Horie, H., Kuwano, H., and Nakagawara, A. (2007) *Genes Cells* **12,** 461–471
27. Miyashita, T., and Reed, J. C. (1995) *Cell* **80,** 293–299
28. Yu, J., Zhang, L., Hwang, P. M., Kinzler, K. W., and Vogelstein, B. (2001) *Mol. Cell* **7,** 673–682
29. Malmlöf, M., Roudier, E., Högberg, J., and Stenius, U. (2007) *J. Biol. Chem.* **282,** 2288–2296
30. Gottlieb, T. M., Leal, J. F., Seger, R., Taya, Y., and Oren, M. (2002) *Oncogene* **21,** 1299–1303
31. Bode, A. M., and Dong, Z. (2004) *Nat. Rev. Cancer* **4,** 793–805
32. Farazi, P. A., and DePinho, R. A. (2006) *Nat. Rev. Cancer* **6,** 674–687
33. Tanaka, T., Inoue, K., Hayashi, Y., Abe, A., Tsukiyama-Kohara, K., Nuriya, H., Aoki, Y., Kawaguchi, R., Kubota, K., Yoshiba, M., Koike, M., Tanaka, S., and Kohara, M. (2004) *J. Med. Virol.* **72,** 223–229
34. Roth, J., Dobbelstein, M., Freedman, D. A., Shenk, T., and Levine, A. J. (1998) *EMBO J.* **17,** 554–564
35. Freedman, D. A., and Levine, A. J. (1998) *Mol. Cell. Biol.* **18,** 7288–7293
36. Kobet, E., Zeng, X., Zhu, Y., Keller, D., and Lu, H. (2000) *Proc. Natl. Acad. Sci. U.S.A.* **97,** 12547–12552
37. Ito, A., Lai, C. H., Zhao, X., Saito, S., Hamilton, M. H., Appella, E., and Yao, T. P. (2001) *EMBO J.* **20,** 1331–1340
38. Ohkubo, S., Tanaka, T., Taya, Y., Kitazato, K., and Prives, C. (2006) *J. Biol. Chem.* **281,** 16943–16950
39. Gu, W., and Roeder, R. G. (1997) *Cell* **90,** 595–606
40. Yuan, Z. M., Huang, Y., Ishiko, T., Nakada, S., Utsugisawa, T., Shioya, H., Utsugisawa, Y., Yokoyama, K., Weichselbaum, R., Shi, Y., and Kufe, D. (1999) *J. Biol. Chem.* **274,** 1883–1886
41. Bonaccorsi, L., Luciani, P., Nesi, G., Mannucci, E., Deledda, C., Dichiara, F., Paglierani, M., Rosati, F., Masieri, L., Serni, S., Carini, M., Proietti-Pannunzi, L., Monti, S., Forti, G., Danza, G., Serio, M., and Peri, A. (2008) *Lab. Invest.* **88,** 1049–1056

JOURNAL OF VIROLOGY, Jan. 2010, p. 303–311 Vol. 84, No. 1
0022-538X/10/$12.00 doi:10.1128/JVI.01448-09

Pathogenesis of Hepatitis C Virus Infection in *Tupaia belangeri*▽†

Yutaka Amako,[1] Kyoko Tsukiyama-Kohara,[1,2] Asao Katsume,[1,3] Yuichi Hirata,[1] Satoshi Sekiguchi,[1] Yoshimi Tobita,[1] Yukiko Hayashi,[4] Tsunekazu Hishima,[4] Nobuaki Funata,[4] Hiromichi Yonekawa,[5] and Michinori Kohara[1]*

Department of Microbiology and Cell Biology, Tokyo Metropolitan Institute of Medical Science, 2-1-6, Kamikitazawa, Setagaya-ku, Tokyo 156-0057, Japan[1]; Department of Experimental Phylaxiology, Faculty of Medical and Pharmaceutical Sciences, Kumamoto University, 1-1-1 Honjo Kumamoto City, Kumamoto 860-8556, Japan[2]; Fuji Gotemba Research Laboratory, Chugai Pharmaceutical Company, Ltd., 135, Komakado 1 Chome, Gotemba-shi, Shizuoka 412-8513, Japan[3]; Department of Pathology, Tokyo Metropolitan Komagome Hospital, 3-18-22 Honkomagome, Bunkyo-ku, Tokyo 113-8677, Japan[4]; and Laboratory of Animal Science, Tokyo Metropolitan Institute of Medical Science, 2-1-6, Kamikitazawa, Setagaya-ku, Tokyo 156-0057, Japan[5]

Received 14 July 2009/Accepted 5 October 2009

The lack of a small-animal model has hampered the analysis of hepatitis C virus (HCV) pathogenesis. The tupaia (*Tupaia belangeri*), a tree shrew, has shown susceptibility to HCV infection and has been considered a possible candidate for a small experimental model of HCV infection. However, a longitudinal analysis of HCV-infected tupaias has yet to be described. Here, we provide an analysis of HCV pathogenesis during the course of infection in tupaias over a 3-year period. The animals were inoculated with hepatitis C patient serum HCR6 or viral particles reconstituted from full-length cDNA. In either case, inoculation caused mild hepatitis and intermittent viremia during the acute phase of infection. Histological analysis of infected livers revealed that HCV caused chronic hepatitis that worsened in a time-dependent manner. Liver steatosis, cirrhotic nodules, and accompanying tumorigenesis were also detected. To examine whether infectious virus particles were produced in tupaia livers, naive animals were inoculated with sera from HCV-infected tupaias, which had been confirmed positive for HCV RNA. As a result, the recipient animals also displayed mild hepatitis and intermittent viremia. Quasispecies were also observed in the NS5A region, signaling phylogenic lineage from the original inoculating sequence. Taken together, these data suggest that the tupaia is a practical animal model for experimental studies of HCV infection.

Hepatitis C virus (HCV) is a small enveloped virus that causes chronic hepatitis worldwide (32). HCV belongs to the genus *Hepacivirus* of the family *Flaviviridae*. Its genome comprises 9.6 kb of single-stranded RNA of positive polarity flanked by highly conserved untranslated regions at both the 5′ and 3′ ends (4, 27, 29). The 5′ untranslated region harbors an internal ribosomal entry site (29) that initiates translation of a single open reading frame encoding a large polyprotein comprising about 3,010 amino acids (35). The encoded polyprotein is co- and posttranslationally processed into 10 individual viral proteins (15).

In most cases of human infection, HCV is highly potent and establishes lifelong persistent infection, which progressively leads to chronic hepatitis, liver steatosis, cirrhosis, and hepatocellular carcinoma (9, 16, 21). The most effective therapy for treatment of HCV infection is administration of pegylated interferon combined with ribavirin. However, the combination therapy is an arduous regimen for patients; furthermore, HCV genotype 1b does not respond efficiently (19). The prevailing scientific opinion is that a more viable option than interferon treatment is needed.

The chimpanzee is the only validated animal model for in vivo studies of HCV infection, and it is capable of reproducing most aspects of human infection (5, 18, 23, 28, 35, 36). The chimpanzee is also the only validated animal for testing the authenticity and infectivity of cloned viral sequences (8, 14, 35, 36). However, chimpanzees are relatively rare and expensive experimental subjects. Cross-species transmission from infected chimpanzees to other nonhuman primates has been tested but has proven unsuccessful for all species evaluated (1).

The tupaia (*Tupaia belangeri*), a tree shrew, is a small nonprimate mammal indigenous to certain areas of Southeast Asia (6). It is susceptible to infection with a wide range of human-pathogenic viruses, including hepatitis B viruses (13, 20, 31), and appears to be permissive for HCV infection (33, 34). In an initial report, approximately one-third of inoculated animals exhibited acute, transient infection, although none developed the high-titer sustained viremia characteristic of infection in humans and chimpanzees (33). The short duration of follow-up precluded any observation of liver pathology. In addition to the putative in vivo model, cultured primary hepatocytes from tupaias can be infected with HCV, leading to de novo synthesis of HCV RNA (37). These reports strongly support tupaias as a valid model for experimental studies of HCV infection. However, longitudinal analyses evaluating the clinical development and pathology of HCV-infected tupaias have yet to be exam-

* Corresponding author. Mailing address: Department of Microbiology and Cell Biology, The Tokyo Metropolitan Institute of Medical Science, 2-1-6, Kamikitazawa, Setagaya-ku, Tokyo 156-0057, Japan. Phone: 81-3-5316-3232. Fax: 81-3-5316-3137. E-mail: kohara-mc@igakuken.or.jp.

† Supplemental material for this article may be found at http://jvi.asm.org/.

▽ Published ahead of print on 21 October 2009.

TABLE 1. Experimental HCV infections performed in this study

Tupaia no.	Inoculum		Biopsy/sacrifice[b]
	Type	Quantity (GE/tupaia)[a]	
Group I[c]			
Tup.4	RCV	1×10^7	84, 94/144 wk p.i.
Tup.5	HCR6	6×10^5	95, 105/155 wk p.i.
Tup.6	HCR6	6×10^5	95, 105/155 wk p.i.
Tup.8	RCV	1×10^7	84, 94/144 wk p.i.
Group II[d]			
Tup.9	Tup.5 (5 wk p.i.)	1×10^2	NT
Tup.10	Tup.5 (5 wk p.i.)	1×10^2	NT
Tup.11	Tup.8 (10 wk p.i.)	1×10^2	NT
Tup.12	Tup.8 (10 wk p.i.)	1×10^2	NT
Tup.13	Tup.4 (8 wk p.i.)	1×10^2	NT
Tup.14	Tup.4 (8 wk p.i.)	1×10^2	NT
Group III[e]			
Tup.15	None		92/100 wk
Tup.17	None		92/100 wk
Tup.38	None		242 wk
Tup.39	None		242 wk

[a] Viral RNA GE/tupaia was estimated by Quantitative real-time RT-PCR (GE, genome equivalents; sensitivity > 10 GE/ml serum).

[b] Liver biopsy was performed at indicated time-point. p.i., postinoculation; NT, not tested.

[c] Group I, primary infection experiment in which 1-year-old animals were inoculated with two different types of inocula.

[d] Group II, reinfection experiment, where HCV RNA-positive sera from Group I experimental infections were passaged to naive animals.

[e] GroupIII, no-infection control.

ined. In the present study, we describe the clinical development and pathology of HCV-infected tupaias over an approximately 3-year time course.

MATERIALS AND METHODS

Animals. Table 1 summarizes the tupaias used in this study. Tupaias born in laboratory captivity were obtained from the Laboratory Animal Center at the Kunming Institute of Zoology (Chinese Academy of Sciences). Tupaias were imported with permission from the Convention on International Trade in Endangered Species of Wild Fauna and Flora (7), quarantined for medical inspection, and housed individually in standard rat cages supplied with filtered air. The animals were fed a daily regimen of eggs, fruit, and the CMS-1 commercial diet for marmosets (CLEA, Japan). Their appetites and feces were carefully monitored. Animal care and experimental handling conformed to study guidelines established by the Subcommittee on Laboratory Animal Care at the Tokyo Metropolitan Institute of Science.

Patient serum used for animal infection. HCV genotype 1b serum, designated HCR6, was obtained from a patient with chronic active hepatitis C. The infectious titer of HCR6 was determined in chimpanzee and Molt4 cells and denoted plasma K (HCR6) by Shimizu et al. (24). The HCR6 serum exhibited a PCR titer of 6×10^6 genome equivalents/ml and an infectious titer of 3.7×10^4 50% chimpanzee infectious doses/ml. Serum aliquots were frozen at −80°C until they were used.

Virion reconstitution of cloned HCV. As described previously, pHCR6 (genotype 1b; 9,611 nucleotides; GenBank accession no. AY045720) is a plasmid carrying HCV genomic cDNA cloned from HCR6 serum (30). pHCR6Rz was designed for precisely trimmed RNA expression, with the entire genomic region of pHCR6Rz recloned under the control of the T7 promoter and the 5′ and 3′ distal ends flanked by hammerhead- and hepatitis D virus ribozyme-encoding sequences, respectively (22, 25).

For molecular reconstitution of HCV particles, pHCR6Rz was transfected into IMY-N9 cells as described previously (12). Briefly, semiconfluent IMY-N9 cells in 100-mm plastic dishes were transfected with 15 μg of plasmid using 40 μl of cationic lipids (DMRIE-C reagent; Life Technology) in accordance with the manufacturer's instructions. Five hours after transfection, the cells were infected with AdexCAT7 (2) (kindly provided by Y. Matsuura) at a multiplicity of infection of 20. After infection, the culture medium was replaced with Hepato-STIM (Becton Dickinson). The culture supernatants were collected at 24 h postinfection and stored at −80°C.

Virus inoculation and collection of serum samples. Animals were infected at 6 months of age. The anesthetic agent, ketamine hydrochloride, was administered intramuscularly at 50 mg/kg body weight prior to virus inoculation and bleeding of the tupaias. The inocula were introduced intravenously at 6×10^5 genome equivalents/animal for patient serum HCR6 and 1×10^7 genome equivalents/animal for reconstituted virions derived from the pHCR6Rz inoculation. Blood samples were drawn from infected and control animals pre- and postinfection. Briefly, the animals were bled weekly for 20 weeks and biweekly thereafter. At each time point, 0.5 ml of blood was drawn from the thigh vein; the sera were separated, aliquoted, and stored for subsequent assays.

Reinfection experiments were performed by transmission of HCV RNA-positive serum from group I (Table 1) to naive animals.

Serum alanine aminotransferase (ALT) concentrations were determined using a Transnase Nissui kit (Nissui Pharmaceutical Co.), standardized, and displayed as IU/liter.

RNA isolation and quantitative RTD-PCR assay for HCV RNA. Serum samples (100 μl) were tested for circulating HCV RNA in vivo using quantitative real-time detection (RTD)-PCR (TaqMan). RNA was extracted from the sera and livers of sacrificed animals using the acid guanidium-phenol chloroform method with tRNA as a carrier (3). Two tupaias (Tup.5 and Tup.6) were inoculated with patient serum HCR6. Another two animals (Tup.4 and Tup.8) were inoculated with reconstituted viral particles (RCV). Tup.15 served as a mock-infected control. Liver specimens (3- to 4-mm^2 blocks) from these tupaias were homogenized with 1.5 ml of 5 M guanidine thiocyanate using a polytron-type homogenizer (Ultra-Turrax T25; IKA Laborteehnik, Staufen, Germany). RNA was then reextracted with 4 M guanidine thiocyanate.

RNA samples were subjected to RTD-PCR on an ABI 7700 sequence detector (Applied Biosystems) as described previously (26). The extracted RNA was dissolved in 200 μl of diethyl pyrocarbonate-treated water containing 10 mM dithiothreitol and 200 units/ml RNase inhibitor in a siliconized tube. RTD-PCR was performed using 1 μg of total RNA, one set of PCR primers, and a probe for a location within the 5′ noncoding region using the EZ *rTth* RNA PCR kit (Perkin Elmer) and the ABI Prism 7700 sequence detector system. A standard curve was constructed using a 10-fold dilution series of in vitro-transcribed and previously titrated synthetic HCV RNA.

Consequently, the quantities represented by genome equivalents correspond to an absolute standard curve (26). All quantitative RTD-PCR assays were performed using duplicate samples, with both negative control serum and HCV-positive serum included. The control sera were diluted before use and were estimated to contain low copy numbers of HCV RNA (100 genome equivalents/ml serum). Samples were deemed positive for HCV RNA if both duplicates yielded PCR-amplified product. Averages of the two estimated values are shown in the figures.

Histological analysis. Tissue samples were carefully collected from anesthetized animals by abdominal incision, fixed in 10% neutral buffered formalin, embedded in paraffin, sectioned, and stained with hematoxylin and eosin (H&E). Silver and Sudan IV (Wako Pure Chemical Industries, Ltd.) staining were also carried out to visualize fiber generation and lipid degeneration, respectively. All histological staining was performed in accordance with conventional procedures. The histological status was determined using the modified hepatitis activity index scoring system, which grades necrosis and inflammation on a scale of 0 to 18 (periportal inflammation and necrosis, 0 to 10; lobular inflammation and necrosis, 0 to 4; portal inflammation, 0 to 4) (11). Fibrosis was scored using the Ishak fibrosis scale of 0 to 6 (0, no fibrosis; 1 or 2, portal fibrosis; 3 or 4, bridging fibrosis; and 5 or 6, cirrhosis). The values in each group (Table 2) represent the averages of the scores in five visual fields.

Statistical analysis. The statistical significance of differences between controls and HCV-infected animals was analyzed with the nonparametric Mann-Whitney U test. All comparisons were two tailed. The statistical analysis was conducted with SPSS 12.0 software (SPSS Inc., Chicago, IL).

RESULTS

Inoculation of HCV causes acute hepatitis and transient viremia in tupaias. To begin this study, two distinct but related inocula were chosen for infection of tupaias. Serum from a chronic hepatitis patient (designated HCR6) was chosen for its

TABLE 2. Grading: necroinflammatory scores and fibrosis

Group	Inoculum	Tupaia no.	Grade				Total	Avg	SD	Staging
			A	B	C	D				
94 wk p.i. (biopsy)										
I	HCR 6	Tup.5	0	0	0	0	0	1.3	1.5	0
		Tup.6	1	0	1	0	2			0
	RCV	Tup.4	0	0	0	0	0			0
		Tup.8	0	0	0	3	3			6
	Control	Tup.15	0	0	0	0	0	0	0	0
III		Tup.17	0	0	0	0	0			0
		Tup.38								
		Tup.39								
144 wk p.i. (sacrifice)										
I	HCR 6	Tup.5	1	0	2	3	6	5.5	3.7	0
		Tup.6	3	0	4	3	10			1
	RCV	Tup.4	0	0	0	1	1			0
		Tup.8	1	0	1	3	5			6
	Control	Tup.15						0	0	
III		Tup.17								
		Tup.38	0	0	0	0	0			0
		Tup.39	0	0	0	0	0			0

defined genotype (genotype 1b), and genetic heterogeneity was ascertained by the process of cloning consensus cDNA. The infectivity of this serum was also experimentally defined in chimpanzees; a 50% chimpanzee infectious dose was estimated at 3.7×10^4 50% chimpanzee infectious doses/ml. Furthermore, the consensus genomic sequence of HCV was cloned from the serum (pHCR6; 9,611 bases; GenBank AY045702.1). For the second inoculum (referred to as RCV), clonal viral particles were reconstituted as described in Materials and Methods. This inoculum was expected to be free of neutralizing antibodies and thus was considered potentially more infectious than patient sera. In the case of RCV infection, genetic diversification of viral RNA, also known as quasispecies, can be regarded as a direct indication of de novo synthesis of progenitor virus in vivo.

Either patient serum or cDNA-derived RCV was inoculated into tupaias (Table 1, group I). Two animals (one female and one male) were tested against each inoculum. Age-matched animals were bred as infection-free controls.

All experimental infections are described in Materials and Methods and Table 1. Prior to experimental infection, the normal serum ALT level in tupaias was measured at 22.3 IU/liter ($n = 23$).

Inoculation with patient serum HCR6 caused rapid fluctuations in the serum ALT concentrations, from two- to fivefold, in both inoculated tupaias, suggesting acute hepatitis in vivo (Fig. 1A and B). Correlative quantitative RTD-PCR revealed HCV viremia soon after serum inoculation in Tup.5, which continued to show transient viremia long term. The appearance of viremia sometimes coincided with a steep elevation in the serum ALT (Fig. 1A). Conversely, HCV RNA was not detected in the serum of Tup.6 up to 60 weeks postinoculation and only twice thereafter. Acute-phase ALT elevations (3 to 4 weeks postinoculation) in Tup.6 might represent tight control of HCV infection by the host immune system (Fig. 1B).

Distinct results were obtained for the two animals (Tup.4 and Tup.8) inoculated with RCV. Both animals displayed sustained viremia up to 10 weeks postinoculation (Fig. 1C and D), indicating persistent HCV infection and inability to eradicate the virus. Viremia was detected intermittently throughout the course of infection, sometimes accompanying the elevation of serum ALT. Humoral immune responses in Tup.5 and Tup.6 (see Fig. S1A in the supplemental material) and Tup.4 and Tup.6 (see Fig. S1B in the supplemental material) were indicated.

We performed RTD-PCR to confirm whether HCV could replicate in the tupaias' livers (Tup.4, Tup.5, Tup.6, and Tup.8) and obtained the following results (Fig. 1E): 310 ± 117 copies/μg total RNA in Tup.5, 80 ± 11 copies/μg in Tup.6, 199 ± 77 copies/μg in Tup.4, and 292 ± 48 copies/μg in Tup.8. In contrast, HCV RNA was not detected in the liver of the mock-infected animal (Tup.15).

HCV RNA was also not detected in samples from either preinoculation or age-matched, infection-free control tupaias (Table 1, group III), nor were significant elevations in serum ALT observed for any of the three infection-free controls (data not shown).

HCV causes chronic hepatitis in tupaia liver, leading to fibrosis and cirrhosis. Serum ALT and circulating HCV RNA levels in primary infected tupaias (Table 1, group I) were monitored for 3 years postinoculation. As described above, the magnitudes of serum ALT fluctuations varied substantially among infected animals (Fig. 1A, B, C, and D). Tupaia livers were examined for histological lesions in order to elucidate if HCV caused chronic hepatitis. Liver biopsies via abdominal incisions were performed at 2 years postinoculation. All animals were sacrificed at 3 years postinoculation (4.5 years for uninfected animals). H&E staining of liver specimens from HCV-infected tupaias showed infiltrating lymphocytes within sinusoids and around portal areas, indicating chronic hepatitis in the tupaia livers (Fig. 2B, D, and H). Infiltrating lymphocytes were also observed in limiting plates, indicating ongoing inflammation (Fig. 2G and H). Furthermore, a comparison of liver samples at 2 and 3 years postinoculation revealed that the

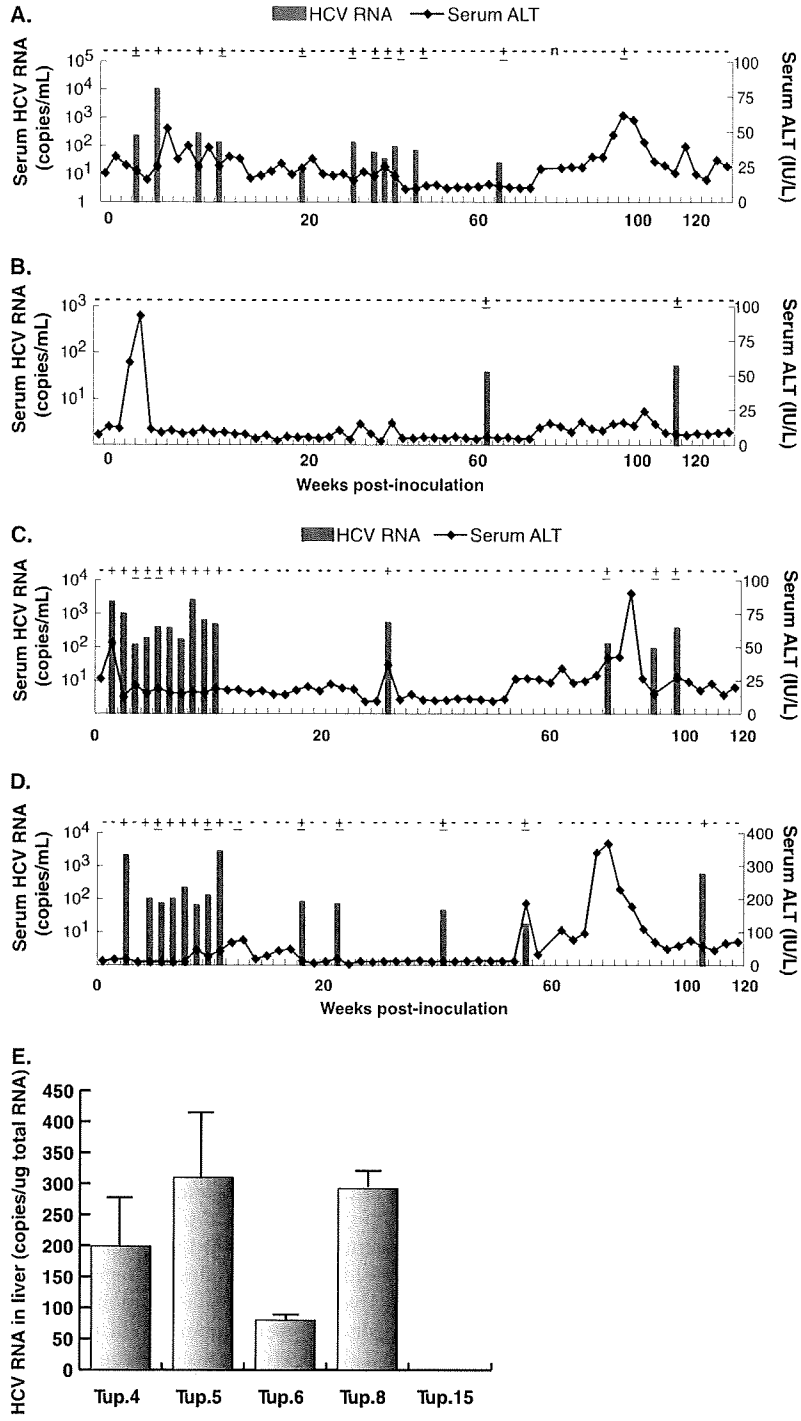

FIG. 1. Course of infection with patient serum HCR6 and RCV. (A) The results of quantitative RTD-PCR for HCV RNA and serum ALT concentrations were combined and plotted to show the course of infection in Tup.5. The bars and the ordinates on the left represent HCV RNA as genome equivalents/ml of serum. The curved line and the ordinates on the right represent serum ALT concentrations as IU/liter serum. (B) Serum HCV RNA and ALT concentrations for infection of Tup.6. (C) The graph for Tup.4. (D) The graph for Tup.8. The vertical axis for serum ALT in this graph is scaled differently from the others because of significant ALT elevation. (E) Quantification of HCV RNA in tupaia liver. HCV RNA in hepatocytes from tupaia (Tup.4, Tup.5, Tup.6, Tup.8, and Tup.15) livers was isolated 172 weeks after HCV infection and quantified by RTD-PCR. As few as 10 copies of the genome were detected, and the quantification range was between 10^1 and 10^8 copies (26).

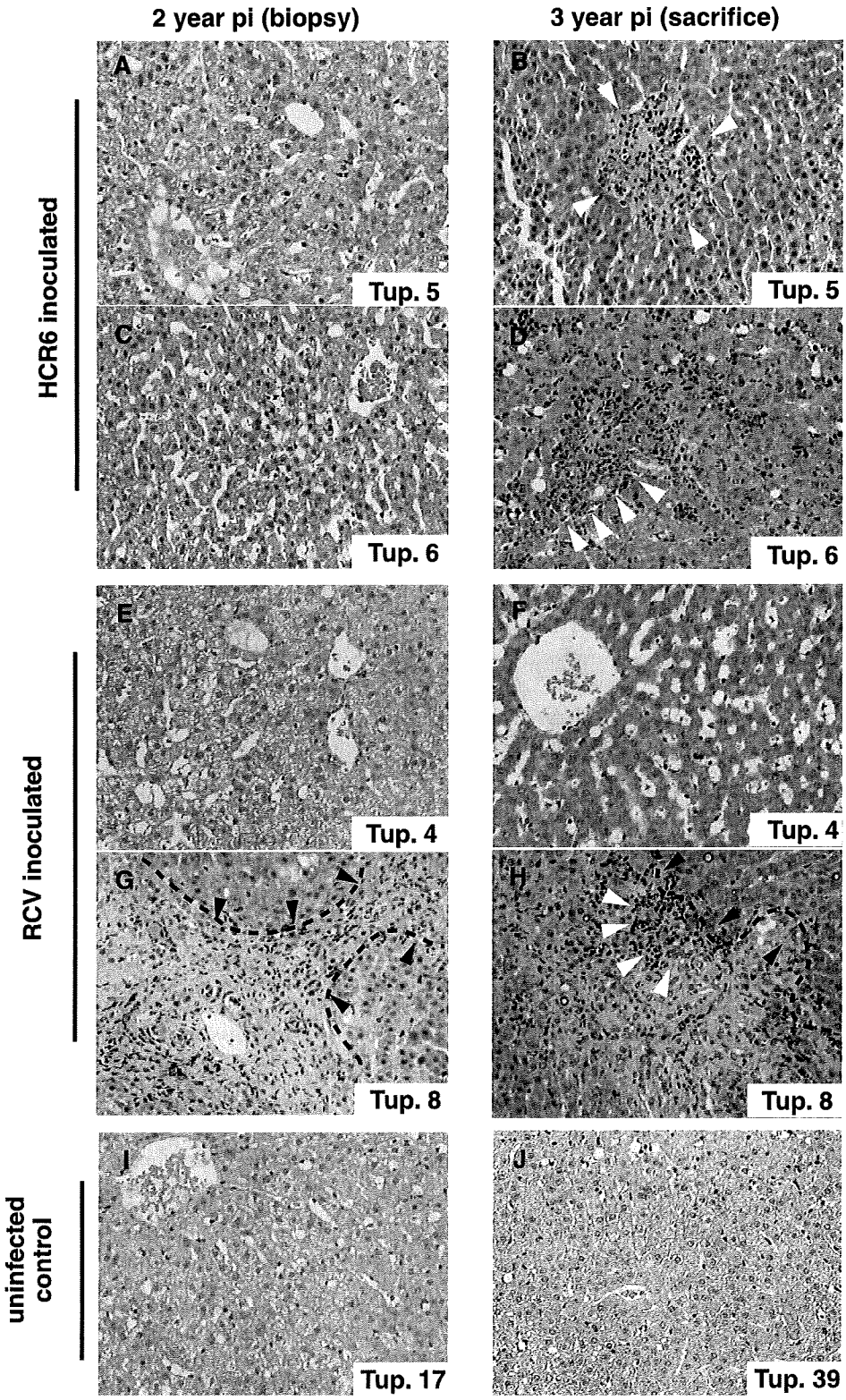

FIG. 2. Micrographs of liver specimens stained with H&E. Liver tissue from HCR6-inoculated tupaias (A to D) and RCV-inoculated tupaias (E to H) was obtained at 2 and 3 years postinoculation (pi). (I and J) Liver specimens from uninfected animals age matched to each inoculated animal were also obtained. The HCV-infected tupaia livers harbored infiltrating lymphocytes (white arrowheads) and fibrosis (broken lines and black arrowheads), which indicate chronic hepatitis.

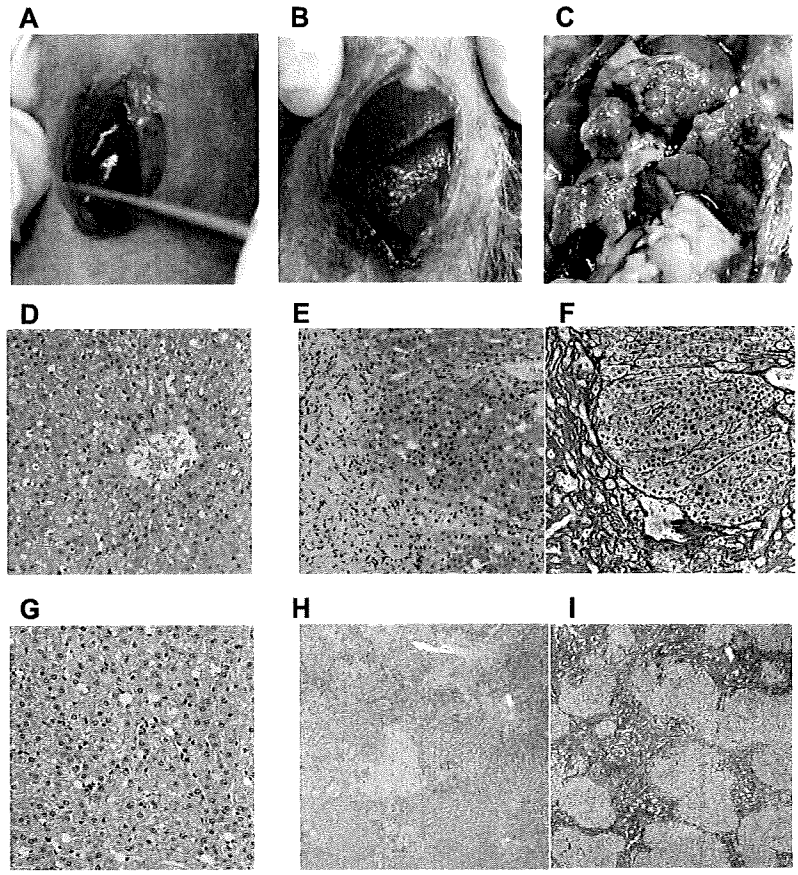

FIG. 3. Macro- and microscopic features of tupaia liver. (A) Infection-free control tupaia (Tup.15; 92 weeks). (B) RCV-infected animal displaying liver cirrhosis (Tup.8; 84 weeks postinoculation). (C) RCV-infected animal with massive surface nodules (Tup.8; 144 weeks postinoculation). (D and G) H&E staining of the uninfected Tup.15 at 92 weeks (D) and the uninfected Tup.39 at 242 weeks (G). (E, F, H, and I) H&E and silver staining of Tup.8 at 84 weeks postinoculation (E and F) or at 144 weeks postinoculation (H and I).

hepatitis had worsened with time in all HCV-infected tupaias (Fig. 2A to H and Table 2).

Fibrosis and cirrhosis were also examined. Mild fibrosis was seen in Tup.6, while severe fibrosis was seen in Tup.8. Cirrhosis was histologically investigated in all animals (Table 2). There was no significant difference between groups I and III at 94 weeks postinfection ($P = 0.194$), but at 144 weeks postinfection, a slight difference was observed ($P = 0.059$; SPSS 12.0). Macroscopic observation of the liver biopsy specimens (taken 2 years postinoculation) indicated liver cirrhosis in Tup.8 (Fig. 3B) compared with Tup.15 (uninfected control) (Fig. 3A), while silver staining of histology samples revealed fibrosis and cirrhotic nodules (Fig. 3E and F). Macroscopic observation upon sacrifice (3 years postinoculation) indicated that liver cirrhosis in Tup.8 had worsened (Fig. 3C). In contrast, age-matched infection-free negative control tupaias displayed none of these pathologies (Fig. 3A, D, and G).

Progressive lipid degeneration was noted in infected tupaias throughout the course of infection (Fig. 4). In particular, Tup.5 displayed microvesicular lipid droplets in the first biopsy specimens (at 2 years), which developed into macrovesicular droplets and foamy degeneration in biopsy specimens at 3 years (Fig. 4C and D). Liver specimens from other infected animals displayed intracellular micro- and macrovesicular lipid droplets in hepatocytes at 3 years postinoculation (Fig. 4F, H, and J). These anomalies were not present in liver specimens from infection-free control animals (Fig. 4A and B).

Transmission of viral-RNA-positive serum to naive animals reproduces acute hepatitis and viremia. To confirm virion regeneration in vivo, and to exclude the possibility of false-positive serum HCV RNA results due to amplification of the original inocula, HCV RNA-positive sera from primary inoculated tupaias were used to inoculate naive tupaias. Three different sera were tested in this passage experiment, with two naive tupaias used as recipient animals for each trial (see Materials and Methods) (Table 1, group II).

In the first reinfection experiment, serum from Tup.5 (originally infected with patient serum HCR6) was collected at 5 weeks postinoculation and used to infect two naive animals. The recipient animals showed intermittent viremia over the subsequent 3 months (Fig. 5A). In the second and third cases of reinfection, sera from Tup.8 at 10 weeks postinoculation and from Tup.4 at 8 weeks postinoculation also induced viremia in the naive inoculated animals, similar to the first reinfection experiment (Fig. 5B and C). Furthermore, the PCR titers of the recipient tupaias were significantly greater than the inoc-

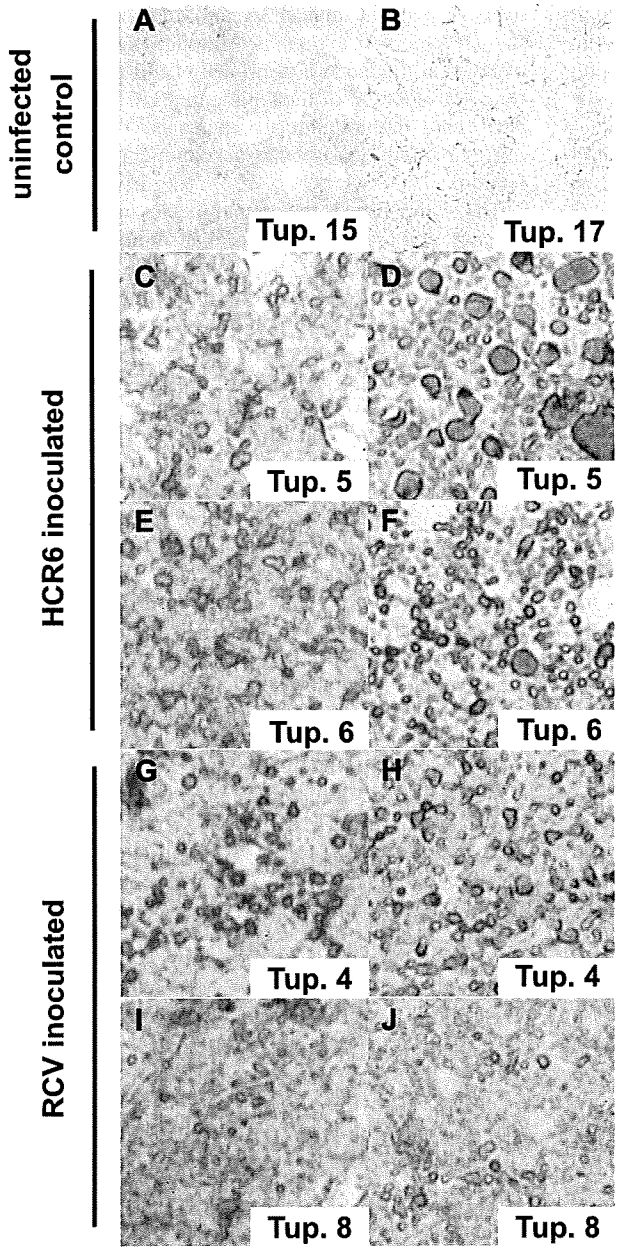

FIG. 4. Sudan IV-stained liver specimens exhibiting fatty liver degeneration. Cryosections of liver stained by Sudan IV as described in Materials and Methods show fatty liver degeneration. The left and right columns display biopsy specimens of infected animals (2 years postinoculation) and animals sacrificed at 3 years postinfection, respectively. (A and B) Uninfected controls at 2 years (Table 1 shows sample timing). (C to F) Patient serum HCR6-infected animals. (G to J) RCV-infected animals.

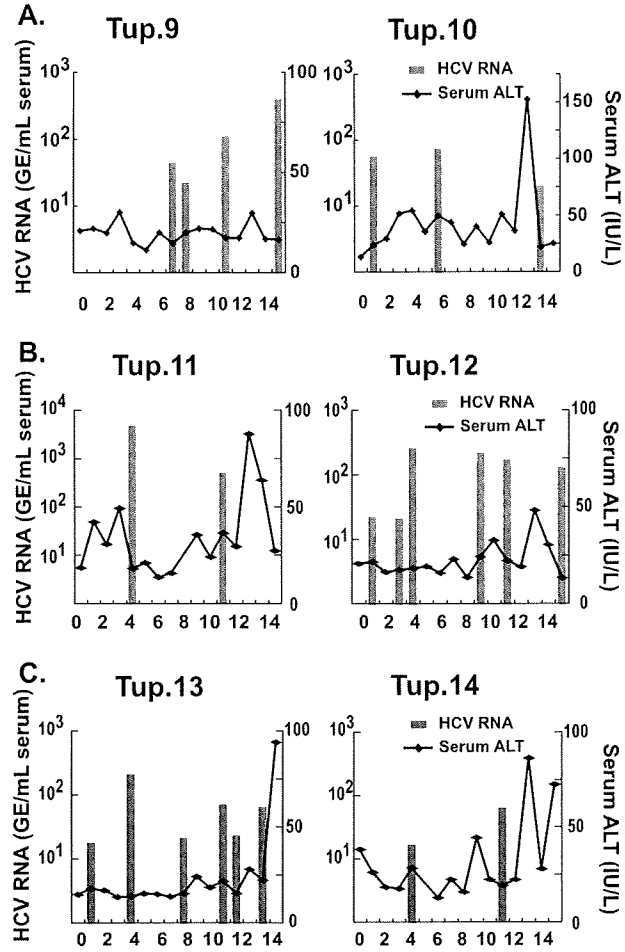

FIG. 5. Results of a reinfection experiment. (A) Quantitative RTD-PCR for HCV RNA and serum ALT levels are shown. Two naive animals were inoculated with tupaia serum (using serum taken at 5 weeks postinoculation from Tup.5, originally inoculated with patient serum HCR6) containing 100 genome equivalents (GE)/ml and were monitored for 15 weeks postinoculation (Table 1). (B) Tupaia serum (taken at 10 weeks postinoculation from Tup.8, originally inoculated with RCV) that was positive for HCV RNA was passaged into two naive animals. The animals were inoculated with tupaia serum at 100 GE/animal and monitored for 15 weeks postinoculation. (C) Tupaia serum (taken at 8 weeks postinoculation from Tup.4, originally inoculated with RCV) that was positive for HCV RNA was passaged into naive animals. The animals were inoculated with serum at 100 GE/animal and monitored for 20 weeks postinoculation.

ulation titers (10^2 genome equivalents/animal) (Table 1). For Tup.11, serum from 4 weeks postinoculation contained almost 10^4 genome equivalents/ml of HCV RNA (Fig. 5B). In addition, significant increases in serum ALT accompanied detection of serum HCV RNA. These results indicate that HCV RNA-positive sera from group I actually contained infectious virion particles. They also suggest that reconstituted HCV particles made from cDNA are infectious in tupaias.

We amplified a portion of the NS5A sequence, which is known as the interferon sensitivity determining region, by reverse transcription-PCR as described in the supplemental material. Each PCR product was subcloned and sequenced to compare the encoded amino acid sequences. For the purposes of this study, animals were inoculated with a molecular clonal virus consisting of a unique viral sequence of cDNA. The interferon sensitivity determining region sequences recovered from an animal infected with clonal inoculum (Tup.8 at 103 weeks postinoculation) were found to be heterogeneous, with

a few amino acid substitutions (K2212M for 2/10 cases, L2232P for 1/10 cases, and L2253S for 6/10 cases) (see Fig. S2E in the supplemental material). Interestingly, the codon for amino acid 2224 encodes valine, but it was found to be variant for alanine and valine in sequences from the original patient serum (HCR6). Tupaias infected with patient serum also exhibited variability at position 2224; valine occupancy was rare, as was seen in the original HCR6 population (see Fig. S2B and C in the supplemental material). On the other hand, this position was occupied solely by valine for sequences recovered from Tup.8 (see Fig. S2E in the supplemental material), indicating that genetic variations shown for Tup.8 originated from the pHCR6 cDNA sequence. Taken together, quasispecies detection of circulating virus represents further evidence demonstrating intrinsic replication of HCV in tupaias despite low levels and infrequent detection of viremia.

DISCUSSION

In the present study, we described persistent HCV infection in tupaias. Long-term follow-up was performed and revealed histological progression of HCV-related liver disorders in infected tupaias, including steatosis, fibrosis, and cirrhosis, in addition to acute and chronic hepatitis. HCV genomic RNA was detected in animal sera intermittently throughout the entire course of infection. However, HCV RNA was detected in the liver upon sacrifice (3 years postinoculation). Furthermore, HCV RNA in serum contained genomic variants that had diverged from the inoculated virus (see Fig. S1 and S2 in the supplemental material). These data strongly indicate an established persistent infection in the tupaias studied. All animals exhibited HCV viremia soon after inoculation, yet the viremia was intermittent and accompanied by relatively low RTD-PCR titers compared with equivalent human and chimpanzee infections. The discrepancy between humans and tupaias might be due to host-dependent differences in replication efficiency. Over the course of HCV infection in these tupaias, serum ALT profiles indicated repeated liver injury, probably due to host immune responses mediated by agents such as cytotoxic T lymphocytes rather than direct viral cytopathic effects.

In cases of tupaia infection, experimental inoculations rarely led to sustained viremia, which for most human cases lasts for the entire course of infection. Even the course of infection appeared transient and self-resolved. It seems likely that HCV replication is less compatible with the tupaia host environment. This possibility was substantiated by a previous report by Xu et al. (34), where tissue-cultured virions of cloned genotype 1b, referred to as HCVcc in the paper, could not cause chronic infection with sustained viremia in tupaias. Although HCVcc actually infected most of the inoculated tupaias (83%; 10/12), chronic infection was seen for only a fraction of them (20%; 2/10). In this study, we also tried to detect a humoral response to HCV core antigen. We found that tupaia sera were HCV positive for antibodies only at occasional time points, observable as intermittent steep responses (data not shown). Overall, sustained seroconversion was not seen in this study, probably because HCV propagation in vivo was so limited or well controlled by host immunity. Given that models of HCV propagation are severely limited, the most important and interesting finding of this study is the successful detection of HCV RNA in livers of infected tupaias 3 years after inoculation, indicating that HCV persists in tupaias. Although the limited propagation of HCV in tupaias is a drawback of this model at the present time, the isolation of tupaia-adapted HCV may be feasible by performing multiple infection passages. This possibility is supported by both quasispecies development and successful reinfection.

The chimpanzee is the animal species most closely related to humans, and as a model, it has contributed significantly to our understanding of HCV infection and pathogenesis. However, reproducing HCV pathogenesis in humans or chimpanzees can take as long as 10 to 20 years. The chronically infected tupaias in the present study developed complicated liver disorders in a much shorter time. Using tupaias, with their relatively short life span (3 to 5 years in the laboratory), as a model of HCV infection, we can evaluate HCV pathogenesis and correlate senescence and duration of infection.

The recent development of a primary human hepatocyte xenograft-uPA/SCID mouse model opened up opportunities to test putative antivirals against HCV replication in vivo (10, 17). In this innovative model, human hepatocytes, which are transplanted into the lobe of a mouse liver, can support HCV replication effectively. As a result, the level of circulating HCV RNA is comparable to that of a human patient. However, this mouse model is immunodeficient, and thus, it lacks the interplay between host immunity and viral infection. Therefore, it does not provide a suitable platform for characterizing immune responses to HCV infection.

HCV infection in tupaias represents an important model of HCV infection, particularly for the study of key determinants controlling virus propagation in vivo. The pathogenesis of HCV infection can be substantially different among humans, chimpanzees, and tupaias, and the mechanisms governing these differences are of great interest. Comparative studies of HCV infection in these different species will help us to understand the basic mechanisms of persistent infection.

ACKNOWLEDGMENTS

We thank Masahiro Shuda for helpful assistance and Etsuko Endo for creating the figures. We also thank the staffs of the Departments of Microbiology and Cell Biology and Mitsugu Takahashi for breeding the tupaias.

This study was supported by grants from the Ministry of Education, Culture, Sports, Science and Technology of Japan; the Program for Promotion of Fundamental Studies in Health Sciences of the Pharmaceuticals and Medical Devices Agency of Japan; and the Ministry of Health, Labor and Welfare of Japan.

REFERENCES

1. **Abe, K., T. Kurata, Y. Teramoto, J. Shiga, and T. Shikata.** 1993. Lack of susceptibility of various primates and woodchucks to hepatitis C virus. J. Med. Primatol. **22**:433–434.
2. **Aoki, Y., H. Aizaki, T. Shimoike, H. Tani, K. Ishii, I. Saito, Y. Matsuura, and T. Miyamura.** 1998. A human liver cell line exhibits efficient translation of HCV RNAs produced by a recombinant adenovirus expressing T7 RNA polymerase. Virology **250**:140–150.
3. **Chomczynski, P., and N. Sacchi.** 1987. Single-step method of RNA isolation by acid guanidinium thiocyanate-phenol-chloroform extraction. Anal. Biochem. **162**:156–159.
4. **Choo, Q. L., G. Kuo, A. J. Weiner, L. R. Overby, D. W. Bradley, and M. Houghton.** 1989. Isolation of a cDNA clone derived from a blood-borne non-A, non-B viral hepatitis genome. Science **244**:359–362.
5. **Dash, S., G. Kalkeri, H. M. McClure, R. F. Garry, S. Clejan, S. N. Thung, and K. K. Murthy.** 2001. Transmission of HCV to a chimpanzee using virus

particles produced in an RNA-transfected HepG2 cell culture. J. Med. Virol. **65**:276–281.
6. **Flugge, P., E. Fuchs, E. Gunther, and L. Walter.** 2002. MHC class I genes of the tree shrew Tupaia belangeri. Immunogenetics **53**:984–988.
7. **Goldsmith, E. I.** 1978. The convention on international trade in endangered species of wild fauna and flora. J. Med. Primatol. **7**:122–124.
8. **Hong, Z., M. Beaudet-Miller, R. E. Lanford, B. Guerra, J. Wright-Minogue, A. Skelton, B. M. Baroudy, G. R. Reyes, and J. Y. Lau.** 1999. Generation of transmissible hepatitis C virions from a molecular clone in chimpanzees. Virology **256**:36–44.
9. **Hoofnagle, J. H.** 2002. Course and outcome of hepatitis C. Hepatology **36**:S21–S29.
10. **Inoue, K., T. Umehara, U. T. Ruegg, F. Yasui, T. Watanabe, H. Yasuda, J. M. Dumont, P. Scalfaro, M. Yoshiba, and M. Kohara.** 2007. Evaluation of a cyclophilin inhibitor in hepatitis C virus-infected chimeric mice in vivo. Hepatology **45**:921–928.
11. **Ishak, K., A. Baptista, L. Bianchi, F. Callea, J. De Groote, F. Gudat, H. Denk, V. Desmet, G. Korb, R. N. MacSween, et al.** 1995. Histological grading and staging of chronic hepatitis. J. Hepatol. **22**:696–699.
12. **Ito, T., K. Yasui, J. Mukaigawa, A. Katsume, M. Kohara, and K. Mitamura.** 2001. Acquisition of susceptibility to hepatitis C virus replication in HepG2 cells by fusion with primary human hepatocytes: establishment of a quantitative assay for hepatitis C virus infectivity in a cell culture system. Hepatology **34**:566–572.
13. **Kock, J., M. Nassal, S. MacNelly, T. F. Baumert, H. E. Blum, and F. von Weizsacker.** 2001. Efficient infection of primary tupaia hepatocytes with purified human and woolly monkey hepatitis B virus. J. Virol. **75**:5084–5089.
14. **Kolykhalov, A. A., E. V. Agapov, K. J. Blight, K. Mihalik, S. M. Feinstone, and C. M. Rice.** 1997. Transmission of hepatitis C by intrahepatic inoculation with transcribed RNA. Science **277**:570–574.
15. **Major, M. E., and S. M. Feinstone.** 1997. The molecular virology of hepatitis C. Hepatology **25**:1527–1538.
16. **Marcellin, P., T. Asselah, and N. Boyer.** 2002. Fibrosis and disease progression in hepatitis C. Hepatology **36**:S47–S56.
17. **Mercer, D. F., D. E. Schiller, J. F. Elliott, D. N. Douglas, C. Hao, A. Rinfret, W. R. Addison, K. P. Fischer, T. A. Churchill, J. R. Lakey, D. L. Tyrrell, and N. M. Kneteman.** 2001. Hepatitis C virus replication in mice with chimeric human livers. Nat. Med. **7**:927–933.
18. **Nascimbeni, M., E. Mizukoshi, M. Bosmann, M. E. Major, K. Mihalik, C. M. Rice, S. M. Feinstone, and B. Rehermann.** 2003. Kinetics of CD4+ and CD8+ memory T-cell responses during hepatitis C virus rechallenge of previously recovered chimpanzees. J. Virol. **77**:4781–4793.
19. **Pawlotsky, J. M.** 2002. Use and interpretation of virological tests for hepatitis C. Hepatology **36**:S65–S73.
20. **Ren, S., and M. Nassal.** 2001. Hepatitis B virus (HBV) virion and covalently closed circular DNA formation in primary tupaia hepatocytes and human hepatoma cell lines upon HBV genome transduction with replication-defective adenovirus vectors. J. Virol. **75**:1104–1116.
21. **Seeff, L. B.** 2002. Natural history of chronic hepatitis C. Hepatology **36**:S35–S46.
22. **Shimayama, T., S. Nishikawa, and K. Taira.** 1995. Generality of the NUX rule: kinetic analysis of the results of systematic mutations in the trinucleotide at the cleavage site of hammerhead ribozymes. Biochemistry **34**:3649–3654.
23. **Shimizu, Y. K., H. Igarashi, T. Kanematu, K. Fujiwara, D. C. Wong, R. H. Purcell, and H. Yoshikura.** 1997. Sequence analysis of the hepatitis C virus genome recovered from serum, liver, and peripheral blood mononuclear cells of infected chimpanzees. J. Virol. **71**:5769–5773.
24. **Shimizu, Y. K., A. Iwamoto, M. Hijikata, R. H. Purcell, and H. Yoshikura.** 1992. Evidence for in vitro replication of hepatitis C virus genome in a human T-cell line. Proc. Natl. Acad. Sci. USA **89**:5477–5481.
25. **Suh, Y. A., P. K. Kumar, K. Taira, and S. Nishikawa.** 1993. Self-cleavage activity of the genomic HDV ribozyme in the presence of various divalent metal ions. Nucleic Acids Res. **21**:3277–3280.
26. **Takeuchi, T., A. Katsume, T. Tanaka, A. Abe, K. Inoue, K. Tsukiyama-Kohara, R. Kawaguchi, S. Tanaka, and M. Kohara.** 1999. Real-time detection system for quantification of hepatitis C virus genome. Gastroenterology **116**:636–642.
27. **Tanaka, T., N. Kato, M. J. Cho, K. Sugiyama, and K. Shimotohno.** 1996. Structure of the 3′ terminus of the hepatitis C virus genome. J. Virol. **70**:3307–3312.
28. **Thomson, M., M. Nascimbeni, M. B. Havert, M. Major, S. Gonzales, H. Alter, S. M. Feinstone, K. K. Murthy, B. Rehermann, and T. J. Liang.** 2003. The clearance of hepatitis C virus infection in chimpanzees may not necessarily correlate with the appearance of acquired immunity. J. Virol. **77**:862–870.
29. **Tsukiyama-Kohara, K., N. Iizuka, M. Kohara, and A. Nomoto.** 1992. Internal ribosome entry site within hepatitis C virus RNA. J. Virol. **66**:1476–1483.
30. **Tsukiyama-Kohara, K., S. Tone, I. Maruyama, K. Inoue, A. Katsume, H. Nuriya, H. Ohmori, J. Ohkawa, K. Taira, Y. Hoshikawa, F. Shibasaki, M. Reth, Y. Minatogawa, and M. Kohara.** 2004. Activation of the CKI-CDK-Rb-E2F pathway in full genome hepatitis C virus-expressing cells. J. Biol. Chem. **279**:14531–14541.
31. **Walter, E., R. Keist, B. Niederost, I. Pult, and H. E. Blum.** 1996. Hepatitis B virus infection of tupaia hepatocytes in vitro and in vivo. Hepatology **24**:1–5.
32. **Wasley, A., and M. J. Alter.** 2000. Epidemiology of hepatitis C: geographic differences and temporal trends. Semin. Liver Dis. **20**:1–16.
33. **Xie, Z. C., J. I. Riezu-Boj, J. J. Lasarte, J. Guillen, J. H. Su, M. P. Civeira, and J. Prieto.** 1998. Transmission of hepatitis C virus infection to tree shrews. Virology **244**:513–520.
34. **Xu, X., H. Chen, X. Cao, and K. Ben.** 2007. Efficient infection of tree shrew (Tupaia belangeri) with hepatitis C virus grown in cell culture or from patient plasma. J. Gen. Virol. **88**:2504–2512.
35. **Yanagi, M., R. H. Purcell, S. U. Emerson, and J. Bukh.** 1997. Transcripts from a single full-length cDNA clone of hepatitis C virus are infectious when directly transfected into the liver of a chimpanzee. Proc. Natl. Acad. Sci. USA **94**:8738–8743.
36. **Yanagi, M., M. St Claire, M. Shapiro, S. U. Emerson, R. H. Purcell, and J. Bukh.** 1998. Transcripts of a chimeric cDNA clone of hepatitis C virus genotype 1b are infectious in vivo. Virology **244**:161–172.
37. **Zhao, X., Z. Y. Tang, B. Klumpp, G. Wolff-Vorbeck, H. Barth, S. Levy, F. von Weizsacker, H. E. Blum, and T. F. Baumert.** 2002. Primary hepatocytes of Tupaia belangeri as a potential model for hepatitis C virus infection. J. Clin. Invest. **109**:221–232.

Oncogene (2007) 26, 5587–5595

www.nature.com/onc

ORIGINAL ARTICLE

Expression of activation-induced cytidine deaminase in human hepatocytes via NF-κB signaling

Y Endo[1], H Marusawa[1], K Kinoshita[2], T Morisawa[1], T Sakurai[1], I-M Okazaki[3], K Watashi[4], K Shimotohno[4], T Honjo[3] and T Chiba[1]

[1]*Department of Gastroenterology and Hepatology, Graduate School of Medicine, Kyoto University, Kyoto, Japan;* [2]*Evolutionary Medicine, Shiga Medical Center Research Institute, Moriyama, Japan;* [3]*Department of Immunology and Genomic Medicine, Graduate School of Medicine, Kyoto University, Kyoto, Japan and* [4]*Laboratory of Human Tumor Viruses, Department of Viral Oncology, Institute for Virus Research, Kyoto University, Kyoto, Japan*

Activation-induced cytidine deaminase (AID) is involved in somatic DNA alterations of the immunoglobulin gene for amplification of immune diversity. The fact that constitutive expression of AID in mice causes tumors in various organs, including lymphoid tissues and lungs, suggests the important role of the aberrant editing activity of AID on various tumor-related genes for carcinogenesis. AID expression, however, is restricted to activated B cells under physiological conditions. We demonstrate here that ectopic AID expression is induced in response to tumor necrosis factor-α stimulation in cultured human hepatocytes. The proinflammatory cytokine-mediated expression of AID is achieved by IκB kinase-dependent nuclear factor (NF)-κB signaling pathways. Hepatitis C virus, one of the leading causes of hepatocellular carcinoma (HCC), enhanced AID expression via NF-κB activation through expression of viral core protein. The aberrant expression of AID in hepatoma-derived cells resulted in accumulation of genetic alterations in the *c-myc* and *pim1* genes, suggesting that inappropriate expression of AID acts as a DNA mutator that enhances the genetic susceptibility to mutagenesis in human hepatocytes. Our current findings indicate that the inappropriate expression of AID is induced by proinflammatory cytokine stimulation and may provide the link between hepatic inflammation and the development of HCC.
Oncogene (2007) **26,** 5587–5595; doi:10.1038/sj.onc.1210344; published online 2 April 2007

Keywords: activation-induced cytidine deaminase; TNF-α; NF-κB; hepatocellular carcinoma; hepatitis C virus; chronic hepatitis

Correspondence: Professor T Chiba, Department of Gastroenterology and Hepatology, Graduate School of Medicine, Kyoto University, 54 Kawara-cho, Shogoin, Sakyo-ku, Kyoto 606-8507, Japan.
E-mail: chiba@kuhp.kyoto-u.ac.jp
Received 13 October 2006; revised 8 January 2007; accepted 15 January 2007; published online 2 April 2007

Introduction

A causal association between inflammation and cancer has been proposed in a variety of chronic inflammatory diseases (Balkwill and Mantovani, 2001; Coussens and Werb, 2002). One of the well-recognized models of inflammation-associated tumor development is human hepatocarcinogenesis, which is closely associated with hepatitis virus-associated chronic liver disease. In fact, epidemiologic studies demonstrate that most human hepatocellular carcinoma (HCC) develops during chronic hepatic inflammation with features of liver cirrhosis or chronic hepatitis (Tsukuma *et al.*, 1993). On the other hand, human cancer develops by a multistep process occurring through the accumulation of gene alterations that govern cell proliferation, regeneration and apoptosis (Lengauer *et al.*, 1998; Loeb *et al.*, 2003). Indeed, DNA mutations leading to the activation of oncogenes and/or inactivation of tumor suppressor genes have been reported in hepatoma cells (Thorgeirsson and Grisham, 2002). The mechanisms of how hepatocytes with underlying chronic inflammation acquire the genetic changes leading to malignant transformation, however, are unknown.

Activation-induced cytidine deaminase (AID) is a member of the cytidine deaminase family (Muramatsu *et al.*, 1999) and is closely related to apolipoprotein B RNA-editing cytidine deaminase 1, which converts cytosine nucleotides to uracils in RNA (Teng *et al.*, 1993). AID is expressed in activated B cells, especially in germinal centers and induces somatic hypermutation (SHM), untemplated point mutations, at a high frequency of 10^{-3}–10^{-4} per base pair, into the variable regions of immunoglobulin genes (Muramatsu *et al.*, 2000; Revy *et al.*, 2000; Kinoshita and Honjo, 2001; Honjo *et al.*, 2002). As overexpression of AID increases the rate of SHM in B-cell lines (Martin *et al.*, 2002) and AID can attack the non-immunoglobulin genes, tight control of this protein activity appears crucial under physiologic conditions (Martin and Scharff, 2002; Okazaki *et al.*, 2002, 2003; Yoshikawa *et al.*, 2002; Kinoshita and Nonaka, 2006). We demonstrated that aberrant AID expression can induce SHM in a non-immunoglobulin gene in nonlymphoid cells (Okazaki

et al., 2002; Yoshikawa *et al.*, 2002), and mice with constitutive expression of AID develop various tumors, including T-cell lymphomas and lung adenomas, suggesting that AID has direct oncogenic potential via the mutagenesis of inappropriate target genes (Okazaki *et al.*, 2003). Notably, we recently revealed that endogenous AID was significantly upregulated in both HCC and surrounding noncancerous liver tissues with underlying cirrhosis or chronic hepatitis, where only minute AID expression is detectable in normal liver (Kou *et al.*, 2007). Moreover, both tumor and non-tumor liver tissues with hepatitis C virus (HCV) infection exhibited significantly higher expression levels of the *AID* gene compared with liver tissues of normal control. These findings led to our hypothesis that aberrant expression of AID is present in hepatocytes and might be involved in the enhanced genetic susceptibility to mutagenesis under inflammatory conditions during hepatocarcinogenesis. We demonstrate here that expression of AID is transcriptionally regulated by nuclear factor (NF)-κB in human hepatocytes, allowing it to induce nucleotide alterations in tumor-related genes. The findings thus provide novel insights into the mechanism of genetic mutations during the process of hepatocarcinogenesis and suggest a link between hepatic inflammation and mutagenesis associated with cancer development.

Results

Development of HCC in AID Tg mice

We previously demonstrated that constitutive expression of AID in transgenic (Tg) mice caused both T-cell lymphoma and micro-adenoma in lung alveoli (Okazaki *et al.*, 2003). In this study, we focused on the impact of AID expression in the liver and thus analysed the liver phenotype of randomly selected AID Tg mice killed between 58 and 84 weeks after birth for pathologic analysis. We found that 4 of 16 (25.0%) Tg mice developed tumors in the liver. Histological examination revealed that those tumors showed a trabecular pattern of growth with focal steatosis, consistent with the morphological appearance of well-differentiated HCC (Figure 1). These findings suggested that aberrant expression of AID in the liver can be genotoxic, leading to the development of HCC.

Endogenous AID is induced in response to proinflammatory cytokines in human hepatocytes

To determine whether proinflammatory cytokines enhance *AID* expression in human hepatocytes, we first analysed the expression of endogenous *AID* transcripts in human hepatoma cell lines by quantitative reverse transcription–polymerase chain reaction (RT–PCR)

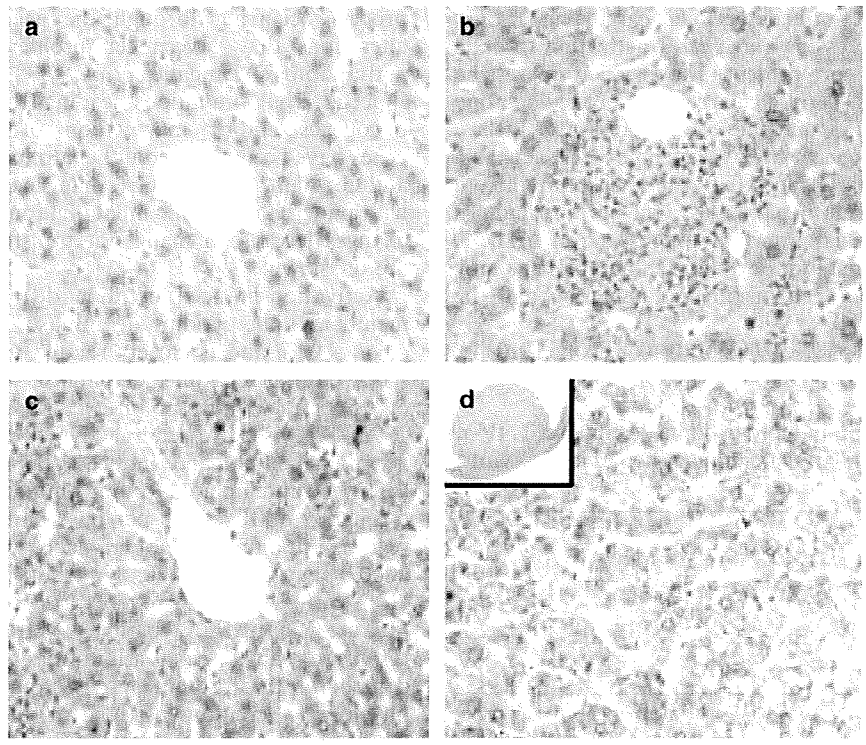

Figure 1 Development of HCC in AID Tg mice. (**a**) H&E-stained sections of the liver of a non-transgenic mouse. (**b**) Liver specimens of the AID Tg mouse with T-cell lymphoma development. Non-tumor region (**c**) and tumor (**d**) of the liver of AID Tg mice with HCC development (original magnification × 400). Insert: a large tumor with extrahepatic growth compressing normal liver tissue was found in a 58-week-old Tg mouse.

using primer sets specific for the human *AID* gene. The expression of *AID* transcripts was undetectable in untreated cells; however, expression of *AID* was induced after the treatment of the cells with tumor necrosis factor (TNF)-α for 10 h (Figure 2a, upper panel). RT–PCR analysis revealed that *AID* transcripts also increased in response to another pro–inflammatory cytokine, interleukin (IL)-1β, in HepG2 cells (Figure 2a, lower panel). To examine whether TNF-α enhances *AID* expression generally in human hepatocytes, we used other hepatoma-derived cell lines, Hep3B and Huh-6. Although both cells lacked the expression of endogenous *AID* transcripts in the resting state, marked upregulation of *AID* transcripts was observed 12–24 h after treatment with TNF-α (Figure 2b), as in HepG2 cells. To confirm the TNF-α-mediated induction of *AID* expression in human hepatocytes, we investigated whether *AID* expression is upregulated by TNF-α stimulation in primary human hepatocytes. Although only trace amounts of endogenous *AID* transcripts were detectable in primary hepatocytes without any stimulation, quantitative RT–PCR analysis revealed a marked upregulation of *AID* transcripts 12 h after treatment with TNF-α (Figure 2c).

To investigate the TNF-α-mediated induction of *AID* more precisely, we examined the time course of *AID* expression by incubating HepG2 cells with TNF-α. *AID* transcripts were promptly induced, and the peak level was observed 8–10 h after TNF-α treatment (Figure 2d). Moreover, TNF-α increased the amount of *AID* transcripts in a dose-dependent manner, whereas the expression of the internal control *18S ribosomal RNA (18S rRNA)* gene was constant under all conditions tested (Figure 2e).

Next, to study the expression of AID protein in hepatocytes, we performed immunoblotting analyses using antibodies specific for human AID (Ta *et al.*, 2003). To confirm the specificity of the antibodies, we used AID-specific small interference RNA (siRNA) to knock down the expression of endogenous AID. Only

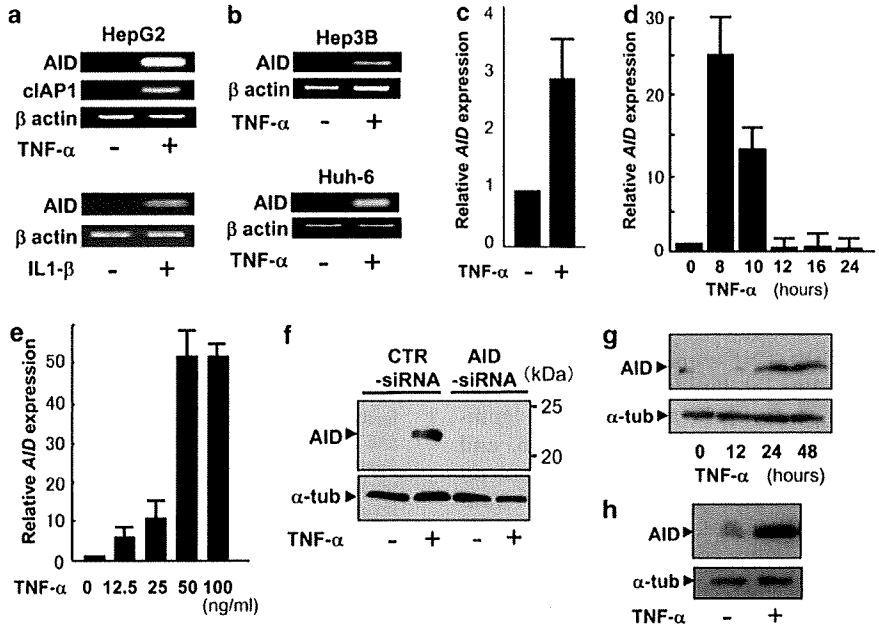

Figure 2 AID expression is induced in human hepatocytes in response to TNF-α and IL-1β stimulation. (**a**) Semiquantitative RT–PCR analyses for *AID* expression in HepG2 cells treated with TNF-α (upper panel) or IL-1β (lower panel). Total RNA was extracted from HepG2 cells after 10 h of treatment with TNF-α (100 ng/ml) or 12 h of treatment with IL-1β (25 ng/ml). Semiquantitative RT–PCR was performed using oligonucleotide primer sets specific for human *AID* and *β-actin*. The expression of *cIAP1*, another TNF-α-inducible gene, was also examined as a control. (**b**) Hep3B and Huh-6 cells were stimulated with TNF-α (100 ng/ml) for 12 h and semiquantitative RT–PCR was performed in each RNA sample using specific primers for *AID* and *β-actin*. (**c**) Human primary hepatocytes were established from surgical specimens of normal liver tissues of patients with metastatic liver tumors. *AID* transcripts were measured with or without TNF-α (12.5 ng/ml) stimulation for 12 h by quantitative real-time RT–PCR and the expression levels of *AID* were normalized to *18S rRNA* as an endogenous control. (**d** and **e**) Time-dependent and dose-dependent effects of TNF-α on *AID* expression. HepG2 cells were treated with TNF-α (100 ng/ml) for the indicated time points (**d**) or with various concentrations of TNF-α (0–100 ng/ml) for 8 h (**e**). Total RNA was extracted from each specimen and subjected to quantitative real-time RT–PCR analyses for *AID* expression. (**f**) HepG2 cells were transfected with siRNA targeting *AID* or control RNA and lysates were prepared from the siRNA-treated cells after stimulation with TNF-α (100 ng/ml) for 24 h. Protein samples were resolved by 15% sodium dodecyl sulfate–polyacrylamide gel electrophoresis. Immunoblotting was performed using antibodies specific for human anti-AID (upper panel) or anti-α-tubulin antibody (α-tub, lower panel). (**g**) HepG2 cells were treated with TNF-α (100 ng/ml) for 0, 12, 24 or 48 h, followed by immunoblotting using anti-AID antibody (upper panel) or anti-α-tubulin antibody (α-tub, lower panel). (**h**) The human primary non-neoplastic hepatocyte cell line was treated with TNF-α (100 ng/ml) for 15 h. Immunoblotting was performed using anti-AID antibody (upper panel) or anti-α-tubulin antibody (α-tub, lower panel).